Title: An OPR3-independent pathway uses 4,5-didehydrojasmonate for jasmonate synthesis.

Authors: Chini A, Monte I, Zamarreño AM, Hamberg M, Lassueur S, Reymond P, Weiss S, Stintzi A, Schaller A, Porzel A, García-Mina JM, Solano R

Journal: Nature chemical biology

Year: 2018 Feb

Issue: 14

Volume: 2

Pages: 171-178

DOI: 10.1038/nchembio.2540

An ORP3-independent pathway uses 4,5-didehydro-jasmonate for jasmonate synthesis

Andrea Chini[1], Isabel Monte[1], Angel M. Zamarreño[2], Mats Hamberg[3], Steve Lassueur[4], Philippe Reymond[4], Sally Weiss[5], Annick Stintzi[5], Andreas Schaller[5], Andrea Porzel[6], José M. García-Mina[2] and Roberto Solano[1]*

[1] Department of Plant Molecular Genetics, National Centre for Biotechnology, Consejo Superior de Investigaciones Científicas (CNB-CSIC), 28049 Madrid, Spain

[2] Environmental Biology Department, University of Navarra, Navarre, Spain

[3] Division of Physiological Chemistry II, Department of Medical Biochemistry and Biophysics, Karolinska Institutte, Stockholm, Sweden

[4] Department of Plant Molecular Biology, University of Lausanne, CH-1015 Lausanne, Switzerland

[5] Institute of Plant Physiology and Biotechnology, University of Hohenheim, 70593 Stuttgart, Germany

[6] Department of Bioorganic Chemistry, Leibniz Institute of Plant Biochemistry, Halle, Germany.

*Corresponding author: rsolano@cnb.csic.es

Key words: OPR1, OPR2, OPR3, jasmonic acid, JA biosynthesis, 4,5-ddh-JA

Abstract

Biosynthesis of the phytohormone jasmonoyl-isoleucine (JA-Ile) requires reduction of the JA precursor 12-oxo-phytodienoic acid (OPDA) by OPDA-reductase-3 (OPR3). Previous analyses of *opr3-1* Arabidopsis mutant suggested an OPDA signaling role, independent of JA-Ile and its receptor COI1; this hypothesis was challenged, as *opr3-1* is a conditional allele not completely impaired in JA-Ile biosynthesis. To clarify the role of OPR3 and OPDA in JA-independent defenses, we isolated and characterized a loss-of-function *opr3-3* allele. Strikingly, *opr3-3* plants remained resistant to necrotrophic pathogens and insect feeding, and activated COI1-dependent JA-mediated gene expression. Analysis of OPDA derivatives identified 4,5-didehydro-JA in wounded wild-type and *opr3-3* plants. OPR2 was found to reduce 4,5-didehydro-JA to JA, explaining the accumulation of JA-Ile and activation of JA-Ile-responses in *opr3-3* mutants. Our results demonstrate that in absence of OPR3 OPDA enters the β-oxidation to produce 4,5-ddh-JA as a direct precursor of JA and JA-Ile, which identifies an OPR3-independent pathway for JA biosynthesis.

Introduction

Jasmonoyl-isoleucine (JA-Ile; **1**), a lipid-derived phytohormone essential for plant survival in nature, regulates plant responses to many stresses including defense against insects, nematodes, and necrotrophic fungal and bacterial pathogens[1-5]. JA-Ile also regulates growth and developmental processes such as pollen viability, stamen development and senescence[5,6]. The bioactive form of the hormone, (+)-7-*iso*-JA-Ile (**2**), acts as "molecular glue" to induce formation of the COI1-JAZ co-receptor complex[7-10]. JA-Ile-mediated COI1-JAZ interaction triggers ubiquitination of JAZ repressors and their degradation by the proteasome, which in turn activates several transcription factors that regulate specific physiological responses[1,7,10].

The octadecanoid pathway is responsible for biosynthesis of JA (**3**) and its derivatives (Supplementary Results, Supplementary Fig. 1)[5,6,11]. Jasmonate biosynthesis begins with release of α-linolenic acid (18:3) from plastidial membrane lipids by lipases and its oxygenation by 13-lipoxygenase[5]. The coupled dehydration-cyclization reaction promoted by allene oxide synthase (AOS) and allene oxide cyclase (AOC) then generates the first cyclopentenone oxylipin, 12-oxo-10,15(*Z*)-phytodienoic acid (OPDA; **4**), in the chloroplast (Supplementary Fig. 1)[5,11]. OPDA is transported into the peroxisome and reduced to 8-(3-oxo-2-(pent-2-enyl)cyclopentyl)octanoic acid (OPC-8) by OPDA reductase 3 (OPR3)[11]. Arabidopsis has at least two additional OPR enzymes, OPR1 and OPR2. Although these enzymes can reduce unnatural stereoisomers of OPDA *in vitro*, experimental evidence of their involvement in OPDA reduction *in vivo* has not been provided yet[12,13]. Peroxisomal OPC-8 undergoes three β-oxidation rounds to generate 6-(3-oxo-2-(pent-2-enyl)cyclopentyl)hexanoic acid (OPC-6), 4-(3-oxo-2-(pent-2-enyl)cyclopentyl)butanoic acid (OPC-4) and finally JA, as an equilibrium of (+)–7-*iso*-JA and (-)-JA stereoisomers[5,14,15]. 2,3-dinor-12-oxo-10,15(*Z*)-phytodienoic acid (dnOPDA; **5**) is a 16-carbon analog of OPDA synthesized from 7,10,13-hexadecatrienoic acid (16:3) by a parallel hexadecanoid pathway

(Supplementary Fig. 1)[5,6,16]. dnOPDA is thought to follow the same pathway as OPDA, giving rise to OPC-6, OPC-4 and JA (Supplementary Fig. 1)[5,6,16]. Finally, the cytoplasmic JA-amido synthetase JAR1 conjugates JA with isoleucine (Ile), to generate bioactive JA-Ile [(+)–7-*iso*-JA-Ile], which is in equilibrium with its inactive epimer (-)-JA-Ile[8,17].

JA biosynthesis or signaling mutants are sterile and more susceptible than wild-type (WT) plants to insects and necrotrophic pathogens. Available *opr3* alleles are also sterile but, in contrast to all other mutants in the pathway, the *opr3-1* allele showed near-WT resistance to insects (i.e., *Bradysia impatiens*) and pathogens (i.e., *Alternaria brassicicola*)[18,19]. This mutant accumulated OPDA, but only minute amounts of JA were detected[19]. A putative role was therefore proposed for OPDA or OPDA derivatives in activation of defenses, independent of JA or other cyclopentanones[19]. Further analysis of the *opr3-1* allele showed it to be a conditional mutant in which the T-DNA insertion in an *OPR3* intron could be spliced out in specific conditions. Upon *Botrytis cinerea* infection, this line produced *OPR3* transcripts, accumulated JA, and showed partial resistance[20]. Although this finding provides a plausible explanation for pathogen resistance in *opr3-1*, the debate remains, since several studies reported JA- or COI1-independent roles for OPDA using tools with certain limitations such as *opr3-1*, RNAi silencing *OPR3*, or weak alleles of *coi1*[21-30]; additional *opr3* alleles described so far do not help in addressing the OPDA role, as they might not be loss-of-function alleles[31].

To further analyze the role of OPR3 and OPDA in defense, we isolated a true loss-of-function *opr3-3* mutant and characterized JA-mediated plant responses. *opr3-3* plants were resistant to insect feeding and necrotrophic pathogen infection, and activated JA-related gene expression in response to these stresses similarly to the original *opr3-1* allele. These responses were fully COI1-dependent and therefore cannot be attributed to the proposed OPDA defense-signaling function. Our data indicate that, in the absence of OPR3, OPDA

could give rise to a COI1 ligand. Quantification of OPDA derivatives showed that *opr3-3* accumulated low JA and JA-Ile levels, which explained the phenotypic observations. In contrast, β-oxidation intermediates such as OPC-6 and OPC-4 were not detected, although we identified 4,5-didehydro-JA (4,5-ddh-JA; **6**) as an alternative jasmonate that accumulated in both WT and *opr3-3* plants. We also showed that 4,5-ddh-JA is not conjugated to Ile to form 4,5-ddh-JA-Ile (**7**), but is reduced to JA by OPR2. Our results define an alternative pathway for JA biosynthesis and demonstrate that OPDA can enter the β-oxidation pathway in the absence of OPR3.

Results

Identification of a knockout (KO) allele of *opr3*

To clarify the controversy generated by the conditional *opr3-1* mutant, we sought a complete loss-of-function *opr3* allele in T-DNA collections. Of the putative mutants selected, only the SK24765 line was sterile (Col-0 background, Saskatoon collection[32]), a well-described feature of *opr3* mutants[18,33]. Exogenous JA restored fertility to SK24765 plants (Fig. 1a). We confirmed T-DNA insertion at position G1982 within the fifth exon in all sterile plants tested, and termed the SK24765 line *opr3-3* (Supplementary Fig. 2a). As anticipated, the *opr3-3* mutation is recessive and heterozygous *opr3-3* plants segregate 1:3 sterile:fertile plants.

To determine whether *opr3-3* was a complete loss-of-function allele, we analyzed *OPR3* expression by qPCR in various conditions including wounding, insect feeding and fungal infections. *opr3-3* did not accumulate any *OPR3* transcripts in any of these conditions (Fig. 1b). Consistent with previous reports[20], however, OPR3 expression was detected in *opr3-1* plants infected by *B. cinerea* and *A. brassicicola* (Supplementary Fig. 2b). These results confirm that the *opr3-1* allele is conditional and indicated that *opr3-3* allele is a complete KO.

opr3-3 activates defense responses

To assess the proposed JA-independent role for OPDA in plant defense, we compared the response of *opr3-3*, WT and *coi1-30* mutants to an insect (*Spodoptera littoralis*), fungal pathogens (*B. cinerea*, *A. brassicicola*) and mechanical wounding. As predicted, *coi1-30* mutants were more susceptible to all pathogens and insect than WT plants, due to the impaired activation of JA-dependent defenses (Fig. 2a and Supplementary Fig. 3). In contrast, *opr3-3* showed near-WT resistance to *B. cinerea* and *A. brassicicola*, not markedly

different from that of the leaky *opr3-1* allele; the *opr3-3* response to *S. littoralis* was intermediate between WT and *coi1-30* (Fig. 2a and Supplementary Fig. 3).

Expression analyses showed that all stress conditions induced several JA marker genes in *opr3-3* mutants (Fig. 2b,c). This induction was lower than in WT plants, but still much higher than the fully impaired induction in *coi1-30* mutants. This finding was unanticipated, as this KO allele was not thought to produce JA, and thus should not activate the JA pathway.

To evaluate whether the defense responses in *opr3-3* depended on the JA-Ile receptor COI1, we generated an *opr3-3 coi1-30* double mutant and challenged it with fungi (*B. cinerea*, *A. brassicicola*), an insect (*S. littoralis*), and wounding. Infection symptoms, spore production, larval weight and induction of defense gene expression for the *opr3-3 coi1-30* mutant were indistinguishable from those of *coi1-30* (Fig. 2 and Supplementary Fig. 3). The data suggest that the complete loss-of-function mutant *opr3-3* can activate JA-mediated gene expression and defense responses in a COI1-dependent manner.

Analysis of JAs in *opr3-3* plants

To understand how *opr3-3* activates JA-mediated responses in a COI1-dependent manner, we measured levels of OPDA-derivatives by liquid chromatography-mass spectrometry (LC-MS) after wounding. Consistent with the KO nature of the *opr3-3* mutation, OPC-4 accumulated in wounded WT but not *opr3-3* plants (Supplementary Fig. 4a). This indicated that lack of a functional OPR3 impairs OPDA reduction, and thus the production of the β-oxidation intermediate OPC-4. The conditional *opr3-1* mutant was very similar to *opr3-3* (Supplementary Fig. 4b).

In contrast to current models of the JA biosynthesis pathway, wounding induced accumulation of low JA and JA-Ile levels in *opr3-3*, similar to the levels reported for the conditional *opr3-1* allele (Fig. 3a-c and Supplementary Fig. 4c,d)[19]. These data suggested the existence of an alternative OPR3-independent pathway for JA biosynthesis.

146 **4,5-didehydro-JA accumulates in *opr3* and WT**

147 In WT plants, OPDA is reduced by OPR3 in the peroxisome and is funneled into the
148 β-oxidation pathway to produce JA. Based on the wide range of molecules that undergo
149 peroxisomal β-oxidation, this process seems to have limited specificity [14,15]. We thus
150 hypothesized that in the absence of OPR3, OPDA might enter the β-oxidation pathway
151 without prior reduction of the cyclopentenone ring to the corresponding cyclopentanone; in
152 this case, it would produce 4,5-didehydrojasmonate (4,5-ddh-JA) as the non-reduced
153 cyclopentenone-analog of JA[34].

154 To test this hypothesis, we chemically synthesized 4,5-ddh-JA and its Ile conjugate 4,5-
155 ddh-JA-Ile (as quantification standards; see Methods and Supplementary Fig. 5a) and
156 analyzed their accumulation in WT and *opr3-3* plants after wounding. WT plants transiently
157 accumulated low 4,5-ddh-JA levels in response to wounding (Fig. 3d), which indicated that
158 the direct entry of OPDA into β-oxidation is a natural alternative in WT plants. *opr3-3*
159 accumulated approximately 20-fold more 4,5-ddh-JA than WT plants after wounding (Fig.
160 3d). The conditional *opr3-1* mutant also accumulated 4,5-ddh-JA at levels similar to *opr3-3*
161 (Supplementary Fig. 6). These data show that 4,5-ddh-JA is a natural oxylipin that
162 accumulates in WT plants in response to wounding, and that this accumulation is promoted in
163 *opr3* alleles. They also suggest that 4,5-ddh-JA is responsible for defense activation in *opr3*
164 alleles. Finally, 4,5-ddh-JA-Ile was not detected in WT or *opr3* plants, which implies that
165 4,5-ddh-JA might not be a JAR1 substrate (Supplementary Fig. 5b).

166 **4,5-didehydro-JA triggers COI1-dependent responses**

167 To assess whether 4,5-ddh-JA acts as a signaling molecule, we analyzed its root-growth
168 inhibitory activity, a typical COI1-mediated response. WT Col-0 plants grown in the
169 presence of 4,5-ddh-JA showed inhibited root growth comparable to that of the JA control
170 treatment (Fig. 4a,b). The *opr3-3* response to 4,5-ddh-JA was similar to that of the WT,

which indicates that this molecule acts downstream of OPR3. Nonetheless, *jar1-1* and *coi1-1* were insensitive to 4,5-ddh-JA, indicating that conjugation to Ile by JAR1 (directly or through conversion to JA) and perception by COI1 are necessary for 4,5-ddh-JA activity (Fig. 4a,b).

We also studied the effect of 4,5-ddh-JA on hormone-induced degradation of JAZ repressors, another typical COI1-mediated response. Both JA and 4,5-ddh-JA rapidly induced JAZ1 protein degradation in Arabidopsis 35S:JAZ1-GUS transgenic plants (Fig. 4c). In addition, 4,5-ddh-JA caused JAZ1-GUS degradation in *opr3-3*, which indicates that OPR3 is not necessary for 4,5-ddh-JA activity. However, neither JA nor 4,5-ddh-JA triggered JAZ1-GUS degradation in *jar1-1* and *coi1-1*, which corroborated the finding that JAR1 is needed to generate the bioactive form of the signaling molecule, which is perceived by COI1. These results show that 4,5-ddh-JA is a signalling molecule that requires JAR1 and COI1 to induce JA-mediated responses.

4,5-didehydro-JA is the source of JA in *opr3-3*

Given that 4,5-ddh-JA was bioactive, but its Ile conjugate could not be detected after wounding, we reasoned that 4,5-ddh-JA might be reduced in the cell to produce JA. To test this hypothesis, we measured JA accumulation after exogenous 4,5-ddh-JA treatment. Both WT and *opr3-3* plants accumulated similarly high JA levels after 4,5-ddh-JA application (Supplementary Fig. 7). To further confirm that 4,5-ddh-JA can be converted to JA, and to detect potential intermediates in this alternative pathway, we fed wounded plants with deuterated α-linolenic acid ([$^2H_5$]18:3) and analyzed accumulation of deuterated 18:3 derivatives. We detected labeled OPDA ([$^2H_5$]OPDA) and dnOPDA ([$^2H_5$]dnOPDA) in WT and *opr3-3* plants (Fig. 5). [$^2H_5$]hexadecatrienoic acid ([$^2H_5$]16:3) was not detected, which shows that [$^2H_5$]dnOPDA is not produced by the parallel hexadecanoid pathway but it is derived from [$^2H_5$]OPDA by a single round of β-oxidation in WT and *opr3-3* plants (Fig. 5b).

The β-oxidation intermediates OPC-6 and OPC-4 were detected as the deuterated derivatives [$^2H_5$]OPC-6 and [$^2H_5$]OPC-4 only in WT but not in *opr3-3* plants (Fig. 5b), which suggests that the canonical β-oxidation of typical OPDA derivatives (OPC) is lost in the absence of OPR3. Both WT and, to a greater extent, *opr3-3* plants accumulated deuterated tetranor-OPDA ([$^2H_5$]tnOPDA; **8**) and 4,5-ddh-JA ([$^2H_5$]4,5-ddh-JA), which implies that dnOPDA can be converted into 4,5-ddh-JA in two further rounds of β-oxidation. Despite the absence of OPC-6 and OPC-4, we detected deuterated JA ([$^2H_5$]JA) and JA-Ile ([$^2H_5$]JA-Ile) in WT and *opr3-3* plants, which indicates that JA can be synthesized by a 4,5-ddh-JA-mediated biosynthetic pathway alternative to the canonical OPC-mediated β-oxidation pathway (Fig. 5b). In summary, these data show that an OPR3-independent JA-biosynthetic pathway occurs naturally in WT plants and that the flux through this pathway is increased in absence of OPR3.

4,5-didehydro-JA is reduced to JA by OPR2

We sought enzymes responsible for conversion of 4,5-ddh-JA to JA in the absence of OPR3. Cytosolic OPR1 and OPR2 are the enzymes most similar to peroxisomal OPR3 [35]. Expression of both *OPR1* and *OPR2* is induced after wounding, although to a lesser extent than *OPR3* (Supplementary Fig. 8a; Genevestigator) [19,36]. To test the hypothesis that OPR1 and OPR2 reduce 4,5-ddh-JA to JA in *opr3-3* plants, loss-of-function *opr1-1* and *opr2-1* mutants were selected and crossed with *opr3-3* to generate the double mutants *opr1-1 opr3-3* and *opr2-1 opr3-3* (Supplementary Fig. 8b-d); triple mutants could not be obtained by crossing, as *OPR1* and *OPR2* are contiguous genes. The single *opr1-1* and *opr2-1* mutants accumulated JA and 4,5-ddh-JA levels similar to those of WT plants after wounding (Fig. 6a,b). Wound-induced levels of 4,5-ddh-JA were as high in *opr1-1 opr3-3* and *opr2-1 opr3-3* as in *opr3-3,* or even slightly higher in *opr2-1 opr3-3* (Figure 6b). In contrast, wound-induced JA accumulation was reduced in *opr1-1 opr3-3* compared to *opr3-3* and almost

undetectable in *opr2-1 opr3-3*, which suggested that OPR2 is the main enzyme responsible for JA reduction from 4,5-ddh-JA (Fig. 6a).

As predicted, JA-Ile accumulation mirrored that of JA. *opr1-1* and *opr2-1* accumulated JA-Ile at levels similar to WT plants. These levels were almost unaffected in *opr1-1 opr3-3* compared to *opr3-3* and undetectable in *opr2-1 opr3-3* (Supplementary Fig. 8e).

To confirm that OPR2 is the main enzymatic activity in 4,5-ddh-JA reduction to JA, we measured JA accumulation after exogenous treatment with 4,5-ddh-JA. *opr3-3* and *opr1-1 opr3-3* plants accumulated similarly high JA and JA-Ile levels after 4,5-ddh-JA application, whereas, the *opr2-1 opr3-3* double mutant showed significantly lower JA and JA-Ile levels (Fig. 6c). These findings show that OPR2 is primarily responsible for JA reduction from 4,5-ddh-JA.

To directly test whether OPR1 and OPR2 are capable of reducing 4,5-ddh-JA to yield JA, the two enzymes were expressed as *N*-terminally His-tagged fusion proteins in *E. coli* and purified from bacterial extracts. Recombinant OPR2 reduced 4,5-ddh-JA at the expense of NADPH with a catalytic efficiency (K_{cat}/K_M) of 3750 $M^{-1}*s^{-1}$ (K_{cat} of 0.819 s^{-1} and V_{max} of 0.819 $M^{-1}*s^{-1}$), while no reduction was observed for OPR1 (Fig. 6d). The apparent K_M of OPR2 for 4,5-ddh-JA, determined as an indirect measure for substrate affinity, was 7-fold higher (218 µM) than the K_M of OPR3 for its substrate OPDA (35 µM)[12]. Therefore, the affinity of OPR2 for 4,5-ddh-JA is lower but in the same order of magnitude to that of OPR3 for OPDA.

To assess the role of OPR1 and OPR2 in pathogen responses, the *opr* double mutants were infected with *B. cinerea* and *A. brassicicola*. As anticipated, *opr3-3* showed near-WT resistance to the fungal infection, very similar to *opr1-1 opr3-3*, whereas *opr2-1 opr3-3* were more susceptible than any of the genetic backgrounds tested (Fig. 6e and Supplementary Fig. 8f-h). Consequently, induction of JA-regulated defence genes was similar in WT and *opr3-3*

246 plants, reduced in *opr1-1 opr3-3* and considerably lower in *opr2-1 opr3-3* (Fig. 6g and
247 Supplementary Fig. 8i).
248 Wound induction of JA-marker gene expression (*JAZ1*, *JAZ5*, *AOS* and *MYC2*) was
249 reduced in the double mutants compared to the single *opr3-3* (Fig. 6h and Supplementary Fig.
250 8j). Induction was also lower in *opr2-1 opr3-3* than *opr1-1 opr3-3*, further suggesting OPR2
251 predominance over OPR1.
252 In all, the genetic, biochemical and physiological data show that OPR2 mediates 4,5-ddh-
253 JA transformation into JA after wounding.
254

Discussion

Here we identify an OPR3-independent pathway for JA biosynthesis that involves direct entry of OPDA into the β-oxidation pathway to produce dnOPDA, tnOPDA and 4,5-ddh-JA, which is then reduced to JA by OPR2. To clarify the controversy regarding the activity of JA precursors in the absence of OPR3 and the role of COI1 in their function, we obtained and characterized a full loss-of-function *opr3-3* allele unable to express any *OPR3* transcript in basal or stress conditions. This knockout mutant was unexpectedly able to activate JA-dependent defenses that were fully dependent on COI1. Consistent with the full KO nature of *opr3-3*, the typical OPDA β-oxidation derivatives and JA precursors OPC-6 and OPC-4 were not detected in this mutant; even so, *opr3-3* accumulated small amounts of JA and JA-Ile in stress situations, which suggested an OPR3- (and OPC)-independent pathway for JA biosynthesis. LC-MS quantification of deuterated derivatives after feeding plants deuterated α-linolenic acid/18:3 showed accumulation of labeled OPDA, dnOPDA, tnOPDA, 4,5-ddh-JA, JA, and JA-Ile in *opr3-3*, but neither OPC-6 nor OPC-4. These results demonstrate that in the absence of OPR3, OPDA can enter the β-oxidation pathway to produce non-reduced OPDA derivatives (dnOPDA, tnOPDA and 4,5-ddh-JA). Labeled dnOPDA, tnOPDA and 4,5-ddh-JA were also identified in WT plants, which indicates that this alternative JA-biosynthetic pathway occurs naturally and is potentiated in the absence of OPR3 in *opr3* mutants.

It was traditionally considered that hexadecatrienoic acid is the only dnOPDA source [16]. Our results indicate that OPDA is an alternative source for dnOPDA production through a single β-oxidation cycle, a conversion that would require OPDA conjugation to CoA. In support of this hypothesis, the OPC8-CoA ligase OPCL1 also accepts OPDA as substrate [37,38]. Moreover, an analysis of Arabidopsis acyl-CoA synthase substrate specificity identified some enzymes with high affinity for OPDA and dnOPDA, and the *At5g63380* gene was proposed

280 to encode an OPDA:CoA ligase [37], although its relevance in JA synthesis remains to be
281 demonstrated. OPDA conversion to OPC-8 by OPR3 was thus thought to occur also at the
282 level of CoA conjugates [37,39]; OPDA-CoA is a high-affinity substrate of the β-oxidation
283 enzyme acyl-CoA oxidase *in vitro*, and direct OPDA entry into β-oxidation has been
284 hypothesized [40].

285 Our genetic analysis of KO mutants complemented the LC-MS quantification and
286 supported 4,5-ddh-JA as the precursor of JA and JA-Ile in *opr3-3*. Previous studies showed
287 that the OPDA reductases OPR1 and OPR2 can reduce OPDA and other oxylipins *in vitro*,
288 but with less efficiency than OPR3 and different stereospecificity [13,14,24,41,42]. This low
289 efficiency, together with the lack of peroxisomal location of OPR1 and OPR2 that contrasts
290 with peroxisomal OPR3, ruled out a role for OPR1 and OPR2 in the JA biosynthetic pathway
291 *in vivo* [13]. Consistent with this idea, we did not detect OPC-6 or OPC-4 in *opr3-3*, which
292 confirmed that OPR1 and OPR2 cannot (even partially) replace OPR3 in OPDA reduction.
293 *opr2* nonetheless show reduced JA accumulation when crossed with *opr3*, which indicates
294 that OPR2 is necessary for 4,5-ddh-JA reduction to JA, likely in the cytoplasm. Confirming
295 the genetic data, recombinant OPR2 was found to catalyze the NADPH-dependent reduction
296 of 4,5-ddh-JA to yield JA. The need for JAR1 for 4,5-ddh-JA activity *in vivo* and the lack of
297 the 4,5-ddh-JA-Ile conjugate also support the concept that 4,5-ddh-JA must be reduced to JA
298 and subsequently conjugated to Ile for activity.

299 Despite the low JA levels detected in the original analysis of *opr3-1* (4% of that in WT) [19]
300 and in more recent studies [43], *opr3-1* has long been assumed to be an appropriate tool for
301 uncoupling OPDA and JA synthesis and for dissecting OPDA-specific responses [5,18,19]. This
302 allele has been widely used to show JA-independent roles of OPDA, which in many cases
303 also seemed to be independent of the JA-Ile receptor COI1 [19,22-29]. *opr3-1* is nonetheless a
304 conditional allele able to express *OPR3* and to produce notable amounts of JA after fungal

infection (up to 30% of JA levels in infected WT plants) [20]. The extensive use of this conditional allele has generated much confusion in the field; therefore, JA-independent functions of OPDA should be revised. This matter was aggravated by the simultaneous use of weak *coi1* alleles, which also suggested COI1-independent functions of OPDA, and by exogenous OPDA treatments that might not represent endogenous functions [22-29].

Our results using *opr3-3 coi1-30* double mutants demonstrate that defense responses in *opr3-3,* including the activation of defense gene expression, are fully COI1-dependent. Although we cannot rule out induction of COI1-independent effects by exogenous OPDA treatment [19,22,24,25,29], OPDA effects that depend on COI1 *in vivo* are unlikely to be mediated by any JA-independent function of OPDA. OPDA-mediated effects that are independent of COI1, on the other hand, may still be attributed to the activity of OPDA per se. The OPDA molecule carries a highly reactive α,β-unsaturated carbonyl group that defines the reactive electrophile species (RES) [44,45]. RES activity induced by exogenous OPDA treatment might thus explain the reported OPDA responses through its binding to cyclophilin 20-3, which in turn regulates cellular redox homeostasis [25].

OPR3 orthologues are not found in lower plants such as Bryophytes, but genes with notable similarity to *OPR2* have been identified [46-49]. Despite of the lack of OPR3, JA and JA-Ile have been detected in several liverworts and mosses, which suggests that the OPR3-independent JA biosynthetic pathway reported here is conserved in lower plants [50]. This alternative *OPR2*-dependent pathway might thus be the original and only way to synthesize JA in ancestral land plants, still present in some extant Bryophytes, whereas the current OPR3-dependence would be a later acquisition in evolution, found only in vascular plants.

Here we identify an OPR3-independent pathway for JA-Ile synthesis that occurs naturally in WT plants and is potentiated in *opr3* mutants. This pathway involves direct peroxisomal β-oxidation of OPDA to dnOPDA, tnOPDA and 4,5-ddh-JA that, after leaving the

330 peroxisome, is reduced to JA in the cytosol by OPR2. That this alternative pathway has a
331 crucial role in certain biological processes or in response to certain environmental stimuli is
332 an attractive hypothesis that awaits further study.
333

Acknowledgements

We thank Vicente Rubio, Jose J. Sánchez-Serrano, Julio Salinas and members of R.S.'s lab for critical reading of the manuscript and Cathy Mark for English editing. Dr. Ulrika Olsson, Karolinska Institutet, is thanked for her assistance with NMR analysis. Work in R.S.'s lab was funded by the Spanish Ministry for Science and Innovation grant BIO2016-77216-R (MINECO/FEDER) and Fundación UAM Grant 2015007. Work in A.S.'s lab was supported by the German Research Foundation (DFG; SCHA 591/6-1, STI 295/2-1).

Author contributions

A.C., M.H., A.Sc., A.St., P.R., J.M. G-M and R.S. designed the experiments, A.C. performed experiments in Figs 1, 2, 4c, 6e,f,g,h, SF2, SF3, SF7 and prepared the material for measurements in Figs 3, 5, 6a,b,c and SF4. I.M. performed experiments in Fig 4a,b. A.M.Z. made metabolite measurements in Figures 3, 5, 6, SF4, SF5, SF6 and SF7. M.H. synthesized all chemicals described in methods. S.L. performed insect assays. S.W. performed experiments in Figure 6d. A.Sc. and A.St. obtained the double *opr* mutants. A.P. recorded NMR data. All authors interpreted the results. A.C. and R.S. wrote the manuscript. All authors edited and commented on the manuscript. R.S. supervised the work.

References

1 Chini, A., Gimenez-Ibanez, S., Goossens, A. & Solano, R. Redundancy and specificity in jasmonate signalling. *Curr Opin Plant Biol* **33**, 147-156, doi:10.1016/j.pbi.2016.07.005 (2016).

2 Fonseca, S., Chico, J. M. & Solano, R. The jasmonate pathway: the ligand, the receptor and the core signalling module. *Curr Opin Plant Biol* **12**, 539-547, doi:10.1016/j.pbi.2009.07.013 (2009).

3 Gimenez-Ibanez, S., Boter, M. & Solano, R. Novel players fine-tune plant trade-offs. *Essays Biochem* **58**, 83-100, doi:10.1042/bse0580083 (2015).

4 Goossens, J., Fernandez-Calvo, P., Schweizer, F. & Goossens, A. Jasmonates: signal transduction components and their roles in environmental stress responses. *Plant Mol Biol* **91**, 673-689, doi:10.1007/s11103-016-0480-9 (2016).

5 Wasternack, C. & Hause, B. Jasmonates: biosynthesis, perception, signal transduction and action in plant stress response, growth and development. An update to the 2007 review in Annals of Botany. *Ann Bot* **111**, 1021-1058, doi:10.1093/aob/mct067 (2013).
6 Acosta, I. F. & Farmer, E. E. Jasmonates. *Arabidopsis Book* **8**, e0129, doi:10.1199/tab.0129 (2010).
7 Chini, A. *et al.* The JAZ family of repressors is the missing link in jasmonate signalling. *Nature* **448**, 666-671, doi:10.1038/nature06006 (2007).
8 Fonseca, S. *et al.* (+)-7-iso-Jasmonoyl-L-isoleucine is the endogenous bioactive jasmonate. *Nat Chem Biol* **5**, 344-350, doi:10.1038/nchembio.161 (2009).
9 Sheard, L. B. *et al.* Jasmonate perception by inositol-phosphate-potentiated COI1-JAZ co-receptor. *Nature* **468**, 400-405, doi:10.1038/nature09430 (2010).
10 Thines, B. *et al.* JAZ repressor proteins are targets of the SCF(COI1) complex during jasmonate signalling. *Nature* **448**, 661-665, doi:10.1038/nature05960 (2007).
11 Schaller, A. & Stintzi, A. Enzymes in jasmonate biosynthesis - structure, function, regulation. *Phytochemistry* **70**, 1532-1538, doi:10.1016/j.phytochem.2009.07.032 (2009).
12 Schaller, F., Biesgen, C., Mussig, C., Altmann, T. & Weiler, E. W. 12-Oxophytodienoate reductase 3 (OPR3) is the isoenzyme involved in jasmonate biosynthesis. *Planta* **210**, 979-984 (2000).
13 Strassner, J. *et al.* Characterization and cDNA-microarray expression analysis of 12-oxophytodienoate reductases reveals differential roles for octadecanoid biosynthesis in the local versus the systemic wound response. *Plant J* **32**, 585-601 (2002).
14 Schaller, F., Schaller, A. & Stintzi, A. Biosynthesis and Metabolism of Jasmonates. *Journal of Plant Growth Regulation* **23**, 179–199, doi:10.1007/s00344-004-0047-x (2004).
15 Baker, A., Graham, I. A., Holdsworth, M., Smith, S. M. & Theodoulou, F. L. Chewing the fat: beta-oxidation in signalling and development. *Trends Plant Sci* **11**, 124-132, doi:10.1016/j.tplants.2006.01.005 (2006).
16 Weber, H., Vick, B. A. & Farmer, E. E. Dinor-oxo-phytodienoic acid: a new hexadecanoid signal in the jasmonate family. *Proc Natl Acad Sci U S A* **94**, 10473-10478 (1997).
17 Staswick, P. E. & Tiryaki, I. The oxylipin signal jasmonic acid is activated by an enzyme that conjugates it to isoleucine in Arabidopsis. *Plant Cell* **16**, 2117-2127, doi:10.1105/tpc.104.023549 (2004).
18 Stintzi, A. & Browse, J. The Arabidopsis male-sterile mutant, opr3, lacks the 12-oxophytodienoic acid reductase required for jasmonate synthesis. *Proc Natl Acad Sci U S A* **97**, 10625-10630, doi:10.1073/pnas.190264497 (2000).
19 Stintzi, A., Weber, H., Reymond, P., Browse, J. & Farmer, E. E. Plant defense in the absence of jasmonic acid: the role of cyclopentenones. *Proc Natl Acad Sci U S A* **98**, 12837-12842, doi:10.1073/pnas.211311098 (2001).
20 Chehab, E. W. *et al.* Intronic T-DNA insertion renders Arabidopsis opr3 a conditional jasmonic acid-producing mutant. *Plant Physiol* **156**, 770-778, doi:10.1104/pp.111.174169 (2011).
21 Bosch, M. *et al.* Jasmonic acid and its precursor 12-oxophytodienoic acid control different aspects of constitutive and induced herbivore defenses in tomato. *Plant Physiol* **166**, 396-410, doi:10.1104/pp.114.237388 (2014).

22 Dave, A. *et al.* 12-oxo-phytodienoic acid accumulation during seed development represses seed germination in Arabidopsis. *Plant Cell* **23**, 583-599, doi:10.1105/tpc.110.081489 (2011).
23 Gleason, C., Leelarasamee, N., Meldau, D. & Feussner, I. OPDA Has Key Role in Regulating Plant Susceptibility to the Root-Knot Nematode Meloidogyne hapla in Arabidopsis. *Front Plant Sci* **7**, 1565, doi:10.3389/fpls.2016.01565 (2016).
24 Mueller, S. *et al.* General detoxification and stress responses are mediated by oxidized lipids through TGA transcription factors in Arabidopsis. *Plant Cell* **20**, 768-785, doi:10.1105/tpc.107.054809 (2008).
25 Park, S. W. *et al.* Cyclophilin 20-3 relays a 12-oxo-phytodienoic acid signal during stress responsive regulation of cellular redox homeostasis. *Proc Natl Acad Sci U S A* **110**, 9559-9564, doi:10.1073/pnas.1218872110 (2013).
26 Ribot, C., Zimmerli, C., Farmer, E. E., Reymond, P. & Poirier, Y. Induction of the Arabidopsis PHO1;H10 gene by 12-oxo-phytodienoic acid but not jasmonic acid via a CORONATINE INSENSITIVE1-dependent pathway. *Plant Physiol* **147**, 696-706, doi:10.1104/pp.108.119321 (2008).
27 Scalschi, L. *et al.* Silencing of OPR3 in tomato reveals the role of OPDA in callose deposition during the activation of defense responses against Botrytis cinerea. *Plant J* **81**, 304-315, doi:10.1111/tpj.12728 (2015).
28 Stotz, H. U. *et al.* Jasmonate-dependent and COI1-independent defense responses against Sclerotinia sclerotiorum in Arabidopsis thaliana: auxin is part of COI1-independent defense signaling. *Plant Cell Physiol* **52**, 1941-1956, doi:10.1093/pcp/pcr127 (2011).
29 Taki, N. *et al.* 12-oxo-phytodienoic acid triggers expression of a distinct set of genes and plays a role in wound-induced gene expression in Arabidopsis. *Plant Physiol* **139**, 1268-1283, doi:10.1104/pp.105.067058 (2005).
30 Raacke, I. C., Mueller, M. J. & Berger, S. Defects in Allene Oxide Synthase and 12-Oxa-Phytodienoic Acid Reductase Alter
the Resistance to *Pseudomonas syringae* and *Botrytis cinerea*. *J. Phytopathology* **154**, 740–744, doi:10.1111/j.1439-0434.2006.01191.x (2006).
31 Acosta, I. F. *et al.* Role of NINJA in root jasmonate signaling. *Proc Natl Acad Sci U S A* **110**, 15473-15478, doi:10.1073/pnas.1307910110 (2013).
32 Robinson, S. J. *et al.* An archived activation tagged population of Arabidopsis thaliana to facilitate forward genetics approaches. *BMC Plant Biol* **9**, 101, doi:10.1186/1471-2229-9-101 (2009).
33 Sanders, P. M. *et al.* The arabidopsis DELAYED DEHISCENCE1 gene encodes an enzyme in the jasmonic acid synthesis pathway. *Plant Cell* **12**, 1041-1061 (2000).
34 Dathe, W. *et al.* Endogenous plant hormones of the broad bean, Vicia faba L. (-)-jasmonic acid, a plant growth inhibitor in pericarp. *Planta* **153**, 530-535, doi:10.1007/BF00385537 (1981).
35 Biesgen, C. & Weiler, E. W. Structure and regulation of OPR1 and OPR2, two closely related genes encoding 12-oxophytodienoic acid-10,11-reductases from Arabidopsis thaliana. *Planta* **208**, 155-165, doi:10.1007/s004250050545 (1999).
36 Delessert, C., Wilson, I. W., Van Der Straeten, D., Dennis, E. S. & Dolferus, R. Spatial and temporal analysis of the local response to wounding in Arabidopsis leaves. *Plant Mol Biol* **55**, 165-181, doi:10.1007/s11103-004-0112-7 (2004).
37 Kienow, L. *et al.* Jasmonates meet fatty acids: functional analysis of a new acyl-coenzyme A synthetase family from Arabidopsis thaliana. *J Exp Bot* **59**, 403-419, doi:10.1093/jxb/erm325 (2008).

38 Koo, A. J., Chung, H. S., Kobayashi, Y. & Howe, G. A. Identification of a peroxisomal acyl-activating enzyme involved in the biosynthesis of jasmonic acid in Arabidopsis. *The Journal of biological chemistry* **281**, 33511-33520, doi:10.1074/jbc.M607854200 (2006).
39 Schneider, K. *et al.* A new type of peroxisomal acyl-coenzyme A synthetase from Arabidopsis thaliana has the catalytic capacity to activate biosynthetic precursors of jasmonic acid. *The Journal of biological chemistry* **280**, 13962-13972, doi:10.1074/jbc.M413578200 (2005).
40 Li, C. *et al.* Role of beta-oxidation in jasmonate biosynthesis and systemic wound signaling in tomato. *Plant Cell* **17**, 971-986, doi:10.1105/tpc.104.029108 (2005).
41 Breithaupt, C. *et al.* Structural basis of substrate specificity of plant 12-oxophytodienoate reductases. *J Mol Biol* **392**, 1266-1277, doi:10.1016/j.jmb.2009.07.087 (2009).
42 Schaller, F., Hennig, P. & Weiler, E. W. 12-Oxophytodienoate-10,11-reductase: occurrence of two isoenzymes of different specificity against stereoisomers of 12-oxophytodienoic acid. *Plant Physiol* **118**, 1345-1351 (1998).
43 Koo, A. J., Gao, X., Jones, A. D. & Howe, G. A. A rapid wound signal activates the systemic synthesis of bioactive jasmonates in Arabidopsis. *Plant J* **59**, 974-986, doi:10.1111/j.1365-313X.2009.03924.x (2009).
44 Farmer, E. E. & Davoine, C. Reactive electrophile species. *Curr Opin Plant Biol* **10**, 380-386, doi:10.1016/j.pbi.2007.04.019 (2007).
45 Farmer, E. E. & Mueller, M. J. ROS-mediated lipid peroxidation and RES-activated signaling. *Annu Rev Plant Biol* **64**, 429-450, doi:10.1146/annurev-arplant-050312-120132 (2013).
46 Han, G. Z. Evolution of jasmonate biosynthesis and signaling mechanisms. *J Exp Bot* **68**, 1323-1331, doi:10.1093/jxb/erw470 (2017).
47 Li, W. *et al.* Phylogenetic analysis, structural evolution and functional divergence of the 12-oxo-phytodienoate acid reductase gene family in plants. *BMC Evol Biol* **9**, 90, doi:10.1186/1471-2148-9-90 (2009).
48 Stumpe, M. *et al.* The moss Physcomitrella patens contains cyclopentenones but no jasmonates: mutations in allene oxide cyclase lead to reduced fertility and altered sporophyte morphology. *New Phytol* **188**, 740-749, doi:10.1111/j.1469-8137.2010.03406.x (2010).
49 Yamamoto, Y. *et al.* Functional analysis of allene oxide cyclase, MpAOC, in the liverwort Marchantia polymorpha. *Phytochemistry* **116**, 48-56, doi:10.1016/j.phytochem.2015.03.008 (2015).
50 Zaveska Drabkova, L., Dobrev, P. I. & Motyka, V. Phytohormone Profiling across the Bryophytes. *PLoS One* **10**, e0125411, doi:10.1371/journal.pone.0125411 (2015).

Figure legends

Figure 1. *opr3-3* is a complete loss-of-function allele

(a) Inflorescences of 7-week-old plants are shown. *opr3-3* mutants are sterile and JA treatment (bracket) rescues male fertility. Scale bars, 1 cm.

(b) Gene expression analysis of *OPR3* in wild-type (Col-0) and *opr3-3* plants in response to *Botrytis cinerea*, *Alternaria brassicicola*, *Spodoptera littoralis*, or wounding. Statistically significant *OPR3* expression differences of control vs. challenged plants (Student's t-test; ** $p < 0.01$ and *** $p < 0.001$). *ACT8* was used as housekeeping control gene. Each biological sample consisted of tissue pooled from 5-10 plants (n = 5). Means ± SD of 4 technical replicates. Each experiment was repeated at least twice with similar results.

Figure 2. *opr3-3* mutants activate defense responses

(a) Box-plots of spore quantification or larval weight of Col-0 plants and mutant infected with *B.cinerea* (n = 15; 3 dai), *A.brassicicola* (n = 15; 9 dai), or challenged with *S.littoralis* larvae (n = 70; 7 dai). Horizontal lines are medians, boxes show the interquartile range and error bars show the full data range. Letters above columns indicate significant differences evaluated by one-way ANOVA/Tukey HSD post hoc test ($p < 0.01$). Experiments were repeated four times with similar results (or twice in the case of Spodoptera).

(b and c) Expression of JA-regulated genes in challenged plants (n = 10). *PDF1.2* and *CYP79B3,* or *JAZ7*, *LOX3* and *AOS* were measured by real-time PCR in untreated plants (control, C) and in plants challenged for 3 days with *B. cinerea* (*Bc*) or 9 days with *A. brassicicola* (*Ab*), or 48 h with *S. littoralis* larvae (*Sl*) or 30 min after wounding. Data in (b) and (c) are shown as mean ± SD (SE in *S.littoralis*) of three technical replicates expressed as relative fold change normalized to *ACT8*. Experiments were repeated three times with similar results. Statistically significant expression differences compared to Col-0 or *opr3-3* are highlighted (Student's t-test; * $p < 0.05$; ** $p < 0.01$; *** $p < 0.001$).

Figure 3. JA accumulation in Col-0 and *opr3-3* plants

(a) Structure of JA-Ile, JA and 4,5,-ddh-JA.

(b) Time-course accumulation of JA (nmoles/fresh weight (g)) in Col-0 (grey bars) and *opr3-3* (black bars) after wounding. Four-week-old plants (n = 10) were wounded, and damaged leaves collected after the indicated time. Data shown as mean ± SD of four biological replicates. Experiments were repeated three times with similar results.

(c) Levels of 4,5-ddh-JA (pmoles/fresh weight (g)) of Col-0 (grey bars) and *opr3-3* (black bars) plants after wounding as in (b) (n = 10). Data shown as mean ± SD of four biological replicates. Experiments were repeated three times with similar results.

(d) Accumulation of JA-Ile (pmoles/fresh weight (g)) in Col-0 (grey bars) and *opr3-3* (black bars) plants after wounding as in (b) (n = 10). Data shown as mean ± SD of four biological replicates. Experiments were repeated three times with similar results.

Figure 4. 4,5-didehydro-JA triggers JA-regulated COI1-dependent responses

(a and b) Arabidopsis Col-0 and mutant seedlings grown for 10 days on control medium (-) or medium supplemented with 50 μM 4,5-ddh-JA (a). Bar, 1 cm. Quantification of root length of Col-0 and mutant seedlings (n = 20) in control medium (-) or medium supplemented with 50 μM JA or 4,5-ddh-JA (b). Data shown as mean ± SD. The experiment was repeated three times with similar results. Letters above columns indicate significant differences (one-way ANOVA/post-hoc Tukey HSD Test, $p < 0.01$).

(c) GUS-staining visualization of JAZ1 stability in roots of 7-day-old transgenic Arabidopsis 35S:JAZ1:GUS on Col-0 or mutant backgrounds. Seedlings were treated with 5 μM JA or 25 μM 4,5-ddh-JA (1 h). The experiment was repeated three times with similar results. Scale bars, 1 mm.

Figure 5. OPDA conversion into 4,5-ddh-JA, JA, and JA-Ile

555 Accumulation (10^6 arbitrary unit/fresh weight (g)) of radiolabeled derivatives of 18:3 in Col-
556 0 and *opr3-3* plants. Five-week-old plants (n = 10) were wounded and fed with deuterated
557 18:3 ([$^2H_5$]18:3) and accumulation of deuterated 18:3 derivatives was analyzed after 30 min.
558 Results shown as means ± SD of four biological replicates. OPDA/dnOPDA biosynthesis
559 takes place in the chloroplasts (top compartment), whereas OPDA/dnOPDA reduction and ®-
560 oxidation occur in the peroxisome (lower compartment). JA is transformed into JA-Ile in the
561 cytosol.

562 **Figure 6. OPR2 converts 4,5-ddh-JA into JA**

563 (a and b) Time-course accumulation of JA or 4,5-ddh-JA in five-week-old Col-0 and *opr*
564 mutants (n = 10) after wounding. Data are shown as mean ± SD of four biological replicates.
565 (c) Accumulation of JA and JA-Ile after exogenous 4,5-ddh-JA treatment in *opr3-3*, *opr1-*
566 *1opr3-3* and *opr2-1opr3-3* mutants (n = 10). Mean ± SD of four biological replicates after
567 subtraction of basal levels.
568 (d) NADPH-dependent reduction of 4,5-ddh-JA by OPR2. The reaction rate (µM*s-1) of
569 recombinant OPR1 and OPR2 (1 µM) was assayed under steady-state conditions with
570 increasing substrate concentrations (10 to 1000 µM of (±)-4,5-ddh-JA). Mean ± SD of three
571 technical replicates.
572 (e) Box-plots of fungal spore quantification of Col-0 and mutant plants (n = 15) infected with
573 *B. cinerea* (7 dai). Letters above columns indicate significant differences (one-way
574 ANOVA/post-hoc Tukey HSD Test, $p < 0.01$).
575 (f) Expression of JA-regulated *PDF1.2* after *B. cinerea* infection or *JAZ5* after wounding in
576 Col-0 and mutant plants (n = 5). Gene expression was measured by RT-qPCR in untreated
577 plants (control, C) and in plants after infection with *B. cinerea* (7 dai) or 1 h after wounding
578 (n = 5). Data shown as mean ± SD of three technical replicates expressed as relative fold
579 change normalized to *ACT8*.

580 Letters above columns in (a), (c), (g), and (h) indicate significant differences compared to
581 expression in *opr3-3* plants (Student's t-test, $p < 0.05$).
582 All experiments were repeated at least twice with similar results.
583

584

585 **Online Methods**

586 **Plant material and growth conditions**

587 *Arabidopsis thaliana* Col-0 is the genetic background of wild-type and mutant lines used
588 in this study, with the exception of *opr3-1*, which is in the Ws background [18]. Plants were
589 grown in Johnson's medium at 21°C in a 16-h light/8-h dark cycle, as described [7,8]. The KO
590 lines *opr1-1* (SALK 145353), *opr2-1* (SALK 116381) and *opr3-3* (SK24765) were obtained
591 from the NASC and the Saskatoon collection [32]. Homozygous lines were selected by PCR
592 using the T-DNA-specific and gene-specific primer combination LB_GW1/OPR3_F1 for
593 *opr3-3*, LBb1.3/OPR1-F1 for *opr1-1* and LBb1.3/OPR2-F1 for *opr2-1*. Double mutants were
594 generated by crossing of single mutant, and double-homozygous plants were identified by
595 PCR analyses. After bolting, flower buds of sterile mutant plants were treated with a 0.5 mM
596 MeJA solution (Sigma) dissolved in 0.1% Tween 20 (Calbiochem), daily for 2 weeks.

597 **Root measurements**

598 For root-growth inhibition assays, root length of 20 to 30 seedlings was measured 10 days
599 after germination, alone or in the presence of 50 μM jasmonic acid (JA; Sigma) or 50 μM 4,5-
600 ddh-JA. Pictures were taken with a Nikon D1-x digital camera and root length was measured
601 using ImageJ software. Data were analyzed by one-way ANOVA/Tukey HSD post hoc test
602 ($p < 0.01$). Three independent biological replicates (20-30 seedlings each) were measured for
603 each sample. Data are shown as mean ± SD.

604 **Fungal infection analyses**

605 Seeds were grown directly in soil as described in [51]. *coi1-30* and *opr3-3 coi1-30* mutants
606 were selected in plates with Johnson's medium containing 0.5 μM coronatine (Sigma), and
607 transferred to soil after 7 days. At least 15 leaves of five-week-old plants (3 leaves/plant)
608 were inoculated with *B. cinerea* suspension of 5×10^6 spores/ml PDB (Difco) as described in

609 [51]. Images of disease symptoms were taken 6 to 9 days after inoculation. Spores were
610 quantified in a hemocytometer under a light microscope (Leica DMR UV/VIS). Five
611 inoculated leaves of five different plants were pooled for each biological sample, and three to
612 seven independent biological replicates were measured for each treatment. Data were
613 analyzed by one-way ANOVA/Tukey HSD post hoc test ($p < 0.01$). This experiment was
614 repeated three times with similar results. Data are shown as mean ± SEM.

615 *A. brassicicola* infection assays were performed as described for *B. cinerea*, inoculating
616 each leaf with 20 µl of a suspension of 10^6 *A. brassicicola* spores/ml PDB. Data (analyzed by
617 one-way ANOVA/Tukey HSD post hoc test, $p < 0.01$) are shown as mean ± SEM. Images of
618 disease symptoms were acquired and spores quantified as for *B. cinerea*.

619 **Insect bioassays**

620 Plants were grown for three weeks in a growth chamber (short-day 10/14h photoperiod,
621 20°C, 65% relative humidity). *coi1-30* and *opr3-3 coi1-30* mutant were selected in the same
622 conditions as for fungal infection assays. Five-week-old plants were placed in transparent
623 plastic boxes and forty newly hatched *Spodoptera littoralis* larvae were placed on 70 plants
624 for seven days of feeding, when larvae were collected and weighed. Data were analyzed on
625 log-transformed values by one-way ANOVA/Tukey HSD post hoc test ($p < 0.01$). The
626 experiment was repeated three times independently, with similar results. Data are shown as
627 mean ± SEM.

628 **Quantitative RT-PCR**

629 Quantitative RT-PCR was performed using biological samples of tissue pooled from 5-10
630 plants. RNA was extracted and purified using Trizol reagent (Invitrogen) followed by the
631 High Pure RNA isolation kit (Roche), including DNase digestion to remove genomic DNA
632 contamination. cDNA was synthesized from 1 µg total RNA with the high-capacity cDNA
633 reverse transcription kit (Applied Biosystems). For gene amplification, 4 µl from a 1:10

cDNA dilution was added to 7.5 μL of Power SYBR Green (Applied Biosystems) and gene-specific primers (Supplementary Table 1). Quantitative PCR was performed in 96-well optical plates in a 7500 or HT 7900 Real Time PCR system (Applied Biosystems) using standard thermocycler conditions (an initial hold at 50°C for 120 s, 95°C for 10 min, followed by a two-step SYBRPCR program of 95°C for 15 s and 60°C for 60 s for 40 cycles). Relative expression values are the mean ± SEM of three to four technical replicates relative to the basal wild-type control using *ACT8* as housekeeping gene. Data were analyzed by unpaired Student's t-test. The experiment was repeated three times independently, with similar results.

Phytohormone analysis

Phytohormone measurements were performed using biological samples of tissue pooled from 5-10 plants and at least three independent biological replicates were measured for each treatment. This experiment was repeated twice or three times with similar results. Data (analyzed by unpaired Student's t-test.) are shown as mean ± SD. (-)-Jasmonic acid (JA), cis-12-oxo-phytodienoic acid (OPDA) and N-(-)-jasmonoyl isoleucine (JA-Ile) were purchased from OlChemim Ltd, dinor-12-oxo-phytodienoic acid (dnOPDA) from Cayman Chemical Company, OPC-4 and OPC-6 described in[8], 4,5-ddh-JA and 4,5-ddh-JA-Ile were synthesized (see below). The deuterium-labeled internal standards $^{2}H_{2}$-N-(-)-jasmonoyl isoleucine ([$^{2}H_{5}$]JA-Ile) and $^{2}H_{5}$-cis-12-oxo-phytodienoic acid ([$^{2}H_{5}$]OPDA) were obtained from OlChemim Ltd., $^{2}H_{5}$-jasmonic acid ([$^{2}H_{5}$]JA) from CDN Isotopes and $^{2}H_{5}$-dinor-12-oxo-phytodienoic acid ([$^{2}H_{5}$]dnOPDA) from Cayman Chemical Co.

Endogenous JA, JA-Ile, OPDA, dnOPDA, OPC-4, OPC-6, tnOPDA, 5-ddh-JA and 4,5-ddh-JA-Ile and the corresponding $^{2}H_{5}$-phytohormones in plants were analyzed using high performance liquid chromatography-electrospray-high-resolution accurate mass spectrometry (HPLC-ESI-HRMS). The hormones were extracted and purified as follows: 0.25 g frozen

plant tissue (ground to a powder in a mortar with liquid N_2) was homogenized with 2.5 ml precooled (-20°C) methanol:water:HCOOH (90:9:1, v/v/v with 2.5 mM Na-diethyldithiocarbamate) and 25 µl of a stock solution of 1000 ng ml^{-1} deuterium-labeled internal standards [$^2H_5$]JA and [$^2H_5$]dnOPDA, 200 ng ml^{-1} [$^2H_5$]JA-Ile and 400 ng ml^{-1} [$^2H_5$]OPDA in methanol. Samples were extracted by shaking in a Multi Reax shaker (Heidolph Instruments) (60 min, 2,000 rpm, room temperature). After extraction, solids were separated by centrifugation (10 min, 20,000 G, room temperature) in a Sigma 4-16K Centrifuge (Sigma Laborzentrifugen), and re-extracted with an additional 1.25 ml extraction mixture, followed by shaking (20 min) and centrifugation. Pooled supernatants (2 ml) were separated and evaporated at 40°C in a RapidVap Evaporator (Labconco Co). The residue was redissolved in 500 µl methanol/0.133% acetic acid (40:60, v/v) and centrifuged (10 min, 20,000 RCF, room temperature) before injection into the HPLC-ESI-HRMS system.

Hormones were quantified using a Dionex Ultimate 3000 UHPLC device coupled to a Q Exactive Focus Mass Spectrometer (Thermo Fisher Scientific) equipped with an HESI(II) source, a quadrupole mass filter, a C-trap, a HCD collision cell and an Orbitrap mass analyzer, using a reverse-phase column (Synergi 4 mm Hydro-RP 80A, 150 x 2 mm; Phenomenex). A linear gradient of methanol (A), water (B) and 2% acetic acid in water (C) was used: 38% A for 3 min, 38% to 96% A in 12 min, 96% A for 2 min and 96% to 38% A in 1 min, followed by stabilization for 4 min. The percentage of C remained constant at 4%. Flow rate was 0.30 ml min^{-1}, injection volume 40 µl, and column and sample temperatures were 35 and 15°C, respectively. Ionization source working parameters were optimized (see Supplementary Table 2).

For phytohormone detection and quantification, we used a full MS experiment with MS/MS confirmation in the negative-ion mode, using multilevel calibration curves with the internal standards. MS^1 extracted from the full MS spectrum was used for quantitative

684 analysis, and MS^2 for confirmation of target identity. For full MS, a m/z scan range from 62
685 to 550 was selected, resolution set at 70,000 full width at half maximum (FWHM), automatic
686 gain control (AGC) target at $1e^6$ and maximum injection time (IT) at 250 ms. A mass
687 tolerance of 5 ppm was accepted. The MS/MS confirmation parameters were resolution of
688 17,500 FWHM, isolation window of 3.0 m/z, AGC target of $2e^5$, maximum IT of 60 ms, loop
689 count of 1 and minimum AGC target of $3e^3$. Instrument control and data processing were
690 carried out with TraceFinder 3.3 EFS software. Accurate masses of phytohormones and
691 internal standard are reported in Supplementary Table 3. Their principal fragments for these
692 molecules are shown in Supplementary Table 3, with the exception of [$^2H_5$]4,5-ddh-JA,
693 [$^2H_5$]ddh-JA-Ile, [$^2H_5$]OPC-4, [$^2H_5$]OPC-6 and [$^2H_5$]tnOPDA.

694 **JAZ1-GUS degradation assays**

695 The 35S:JAZ1-GUS in wild-type and *coi1-30* background were described [10,52]. The
696 35S:JAZ1-GUS marker line was introgressed into *opr3-3* and *jar1-1* backgrounds by crossing,
697 and double homozygous lines were used for further analyses. 35S:JAZ1-GUS seedlings were
698 grown vertically on MS plates and 6-day-old seedlings were treated for 1 h with jasmonate
699 solution as described [53]. To visualize GUS activity, samples were placed in staining solution
700 and incubated (overnight, 37°C) as described in [53]. Tissue was then soaked several times in
701 75% ethanol and kept in 5% glycerol for photography with a Nikon D1-x camera. The
702 analysis was performed using 5-15 plants per sample. This experiment was repeated at least
703 three times with similar results.

704 **Analysis of OPR1 and OPR2 activity**

705 The open reading frames of Arabidopsis OPR1 and OPR2 were previously cloned into the
706 expression vectors pQE-30 and pQE-31 (Qiagen) and kindly provided by Florian Schaller
707 [12,54]. For protein expression, an over-night culture of the expression constructs in *E. coli*
708 BL21-CodonPlus (DE3)-RIL (Agilent Technologies) was used to inoculate 400 mL LB

medium to an OD_{600} of 0.01. The culture was grown at 37°C to OD_{600} of 0.8, when protein expression was induced by addition of 1 mM isopropyl-1-thio-β-D-galactopyranoside. After 4 h at 30°C, cells were harvested by centrifugation and lysed in BugBuster (5 mL per gram packed cell weight; Merck Life Science) containing 1 mM PMSF. The lysates were cleared by centrifugation (20000 xg, 20 min, 4°C), recombinant OPRs were purified by metal chelate affinity chromatography on Ni-nitrilotriacetate (Ni-NTA) agarose (Qiagen) following the supplier's protocols, and dialyzed against 25 mM Tris/HCl pH 7.5. The concentration of OPR1 and OPR2 was determined spectrophotometrically at 445 nm using a molar extinction coefficient of $\varepsilon_{445} = 11600\ M^{-1}cm^{-1}$.

Activity of OPR1 or OPR2 was measured spectrophotometrically by recording NADPH consumption at 340 nm in disposable UV micro cuvettes. Activity assays were performed under steady state conditions at 25°C in 0.2 mL 50 mM Na_2HPO_4/NaH_2PO_4 buffer pH 7.0 containing 0.1 % (v/v) Triton X-100 and 20 mM glucose/1 U/µL glucose oxidase as an oxygen consuming system. Reaction mixtures contained recombinant OPR1 or OPR2 at a concentration of 1 µM, 200 µM NADPH, and the racemate (±)-4,5-didehydro-jasmonic acid at a range of concentrations from 10 µM to 1 mM. This racemate includes natural and unnatural *trans* isomers. Apparent kinetic constants were derived by fitting the data to the Michaelis-Menten equation by the non-linear least squares method using the Enzyme Kinetics module 1.3 of the Sigmaplot version 10.0 (Systat Software GmbH). Assays were performed using three technical replicates and data are shown as mean ± SD. This experiment was repeated twice with similar results.

Online Methods References

51 Gimenez-Ibanez, S. *et al.* JAZ2 controls stomata dynamics during bacterial invasion. *New Phytol* **213**, 1378-1392, doi:10.1111/nph.14354 (2017).

52 Monte, I. *et al.* Rational design of a ligand-based antagonist of jasmonate perception. *Nat Chem Biol* **10**, 671-676, doi:10.1038/nchembio.1575 (2014).
53 Chini, A. Application of yeast-two hybrid assay to chemical genomic screens: a high-throughput system to identify novel molecules modulating plant hormone receptor complexes. *Methods Mol Biol* **1056**, 35-43, doi:10.1007/978-1-62703-592-7_4 (2014).
54 Schaller, F. & Weiler, E. W. Molecular cloning and characterization of 12-oxophytodienoate reductase, an enzyme of the octadecanoid signaling pathway from *Arabidopsis thaliana*. Structural and functional relationship to yeast old yellow enzyme. *J. Biol. Chem.* **272**, 28066-28072 (1997).

Data Availability

All data generated or analysed during this study are included in this published article (and its supplementary information files).

Supplementary Results

Supplementary Fig. 1. Biosynthesis and intracellular flux of jasmonates in Arabidopsis

Supplementary Fig. 2. *opr3* mutants in Arabidopsis

Supplementary Fig. 3. Responses of *opr3* mutants to fungal infection

Supplementary Fig. 4. Accumulation of JA derivatives in wild-type plants and *opr3* mutants

Supplementary Fig. 5. Structures of 4,5-ddh-JA and 4,5-ddh-JA-Ile

Supplementary Fig. 6. Accumulation of 4,5-ddh-JA in wild-type plants and *opr3* plants

Supplementary Fig. 7. Analysis of *OPR* expression and characterization of *opr* mutants

Supplementary Table 1. List of primers used

Supplementary Table 2. Ionization source working parameters

Supplementary Table 3. Masses of phytohormones and internal standard and their principal fragments

764

765

766

767 **Competing financial interests statement**

768 The corresponding author declares on behalf of all co-authors that there are no competing

769 financial interests.

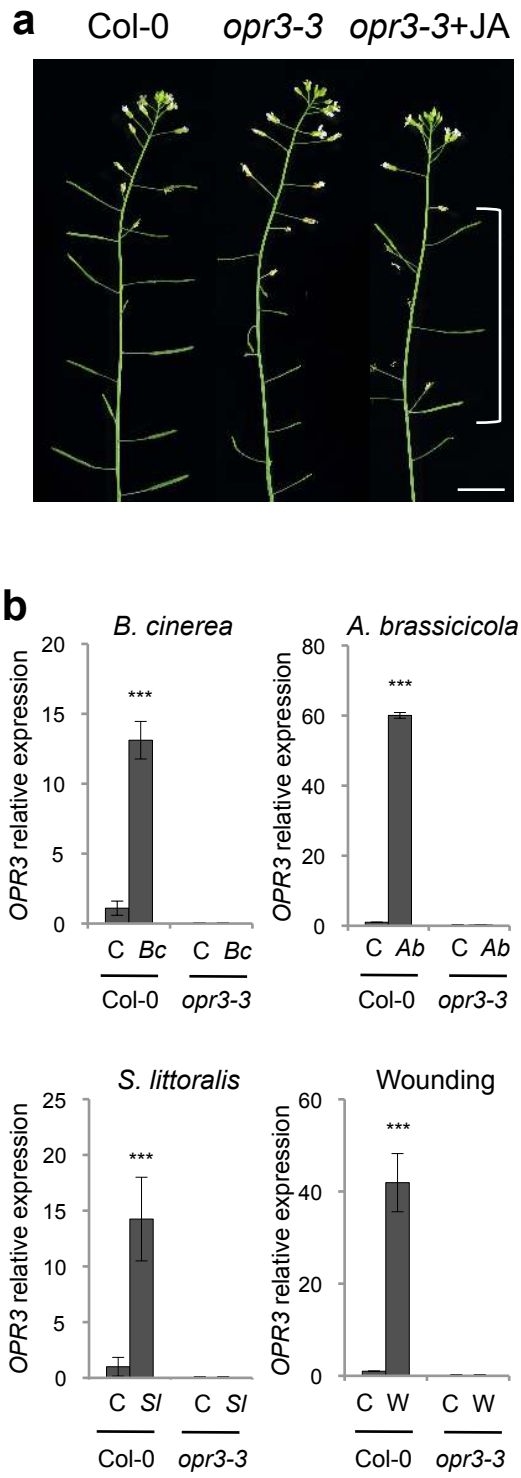

Figure 1. *opr3-3* is a complete loss-of-function allele

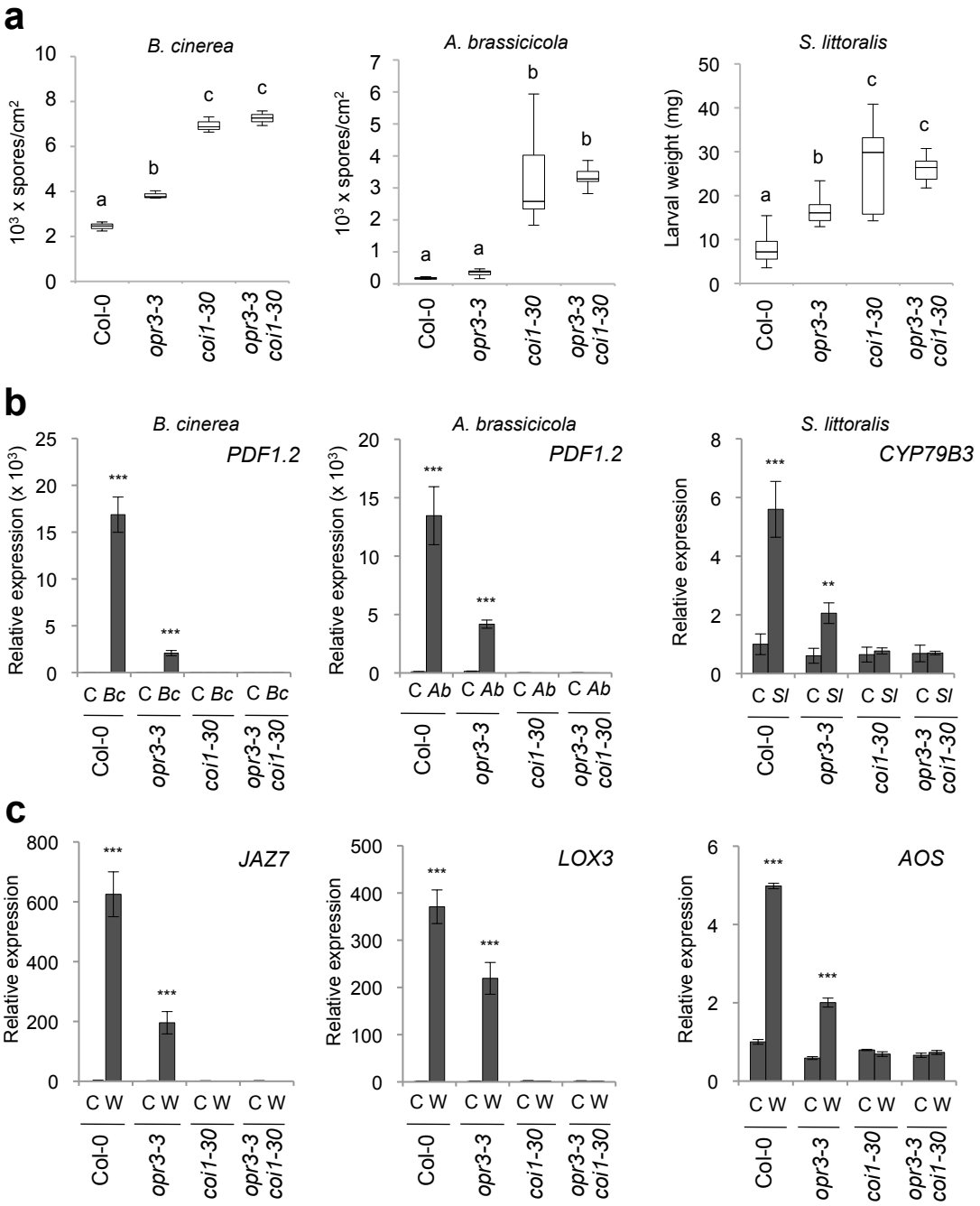

Figure 2. *opr3-3* mutants activate defense responses

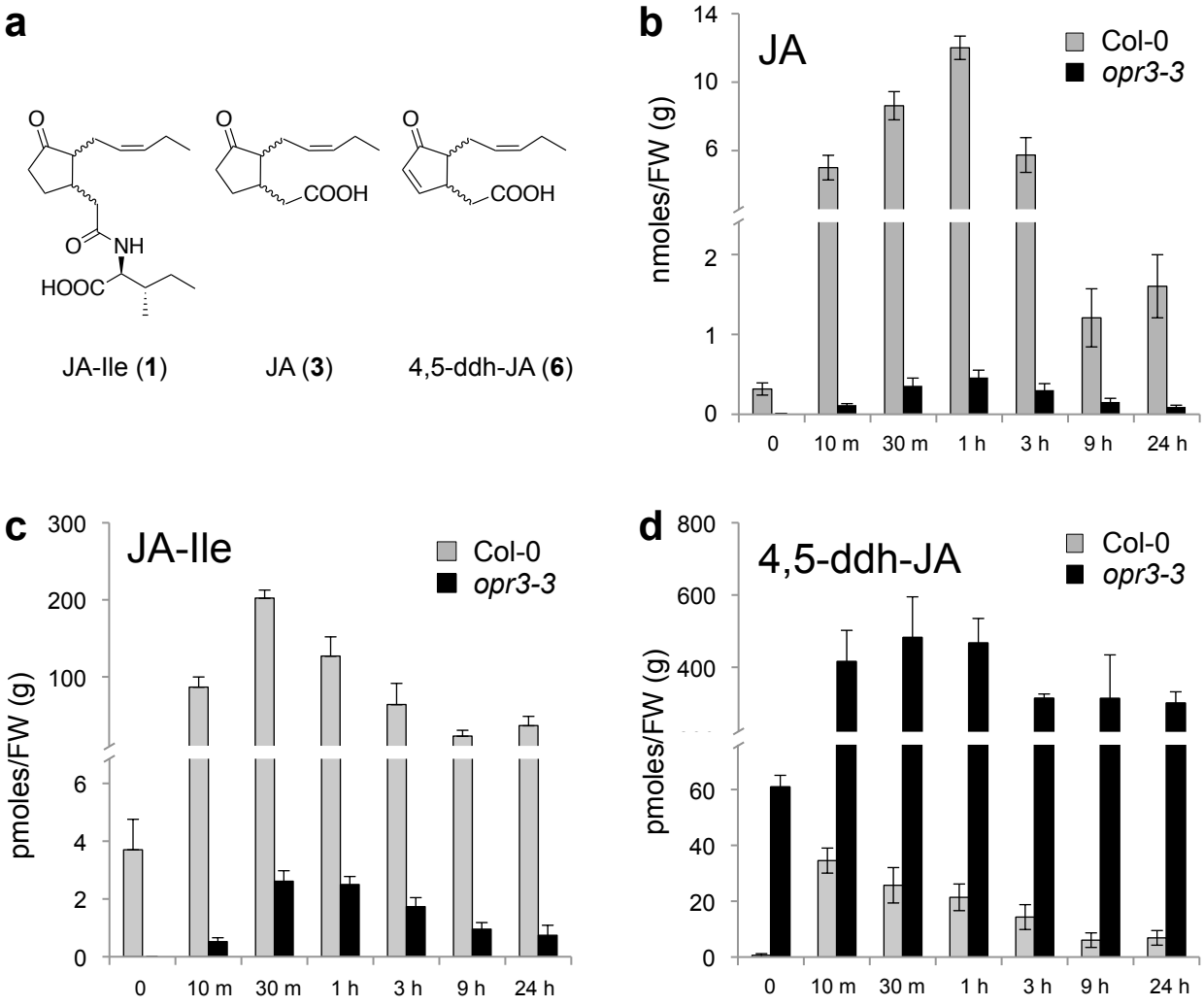

Figure 3. JA accumulation in Col-0 and *opr3-3* plants

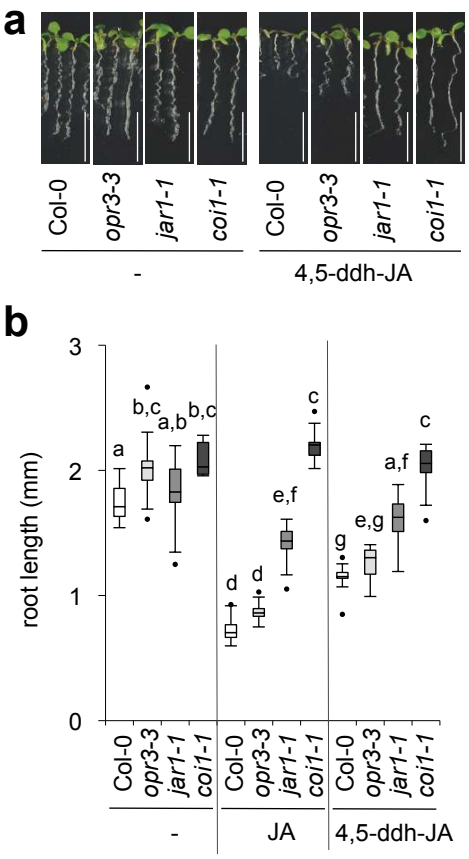

Figure 4. 4,5-didehydro-JA triggers JA-regulated COI1-dependent responses

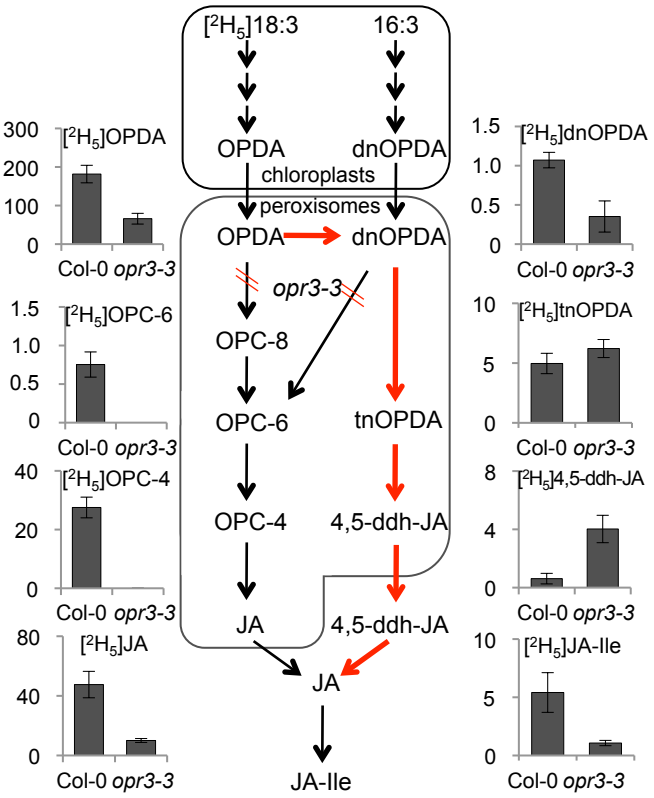

Figure 5. OPDA convention into 4,5-ddh-JA, JA, and JA-Ile

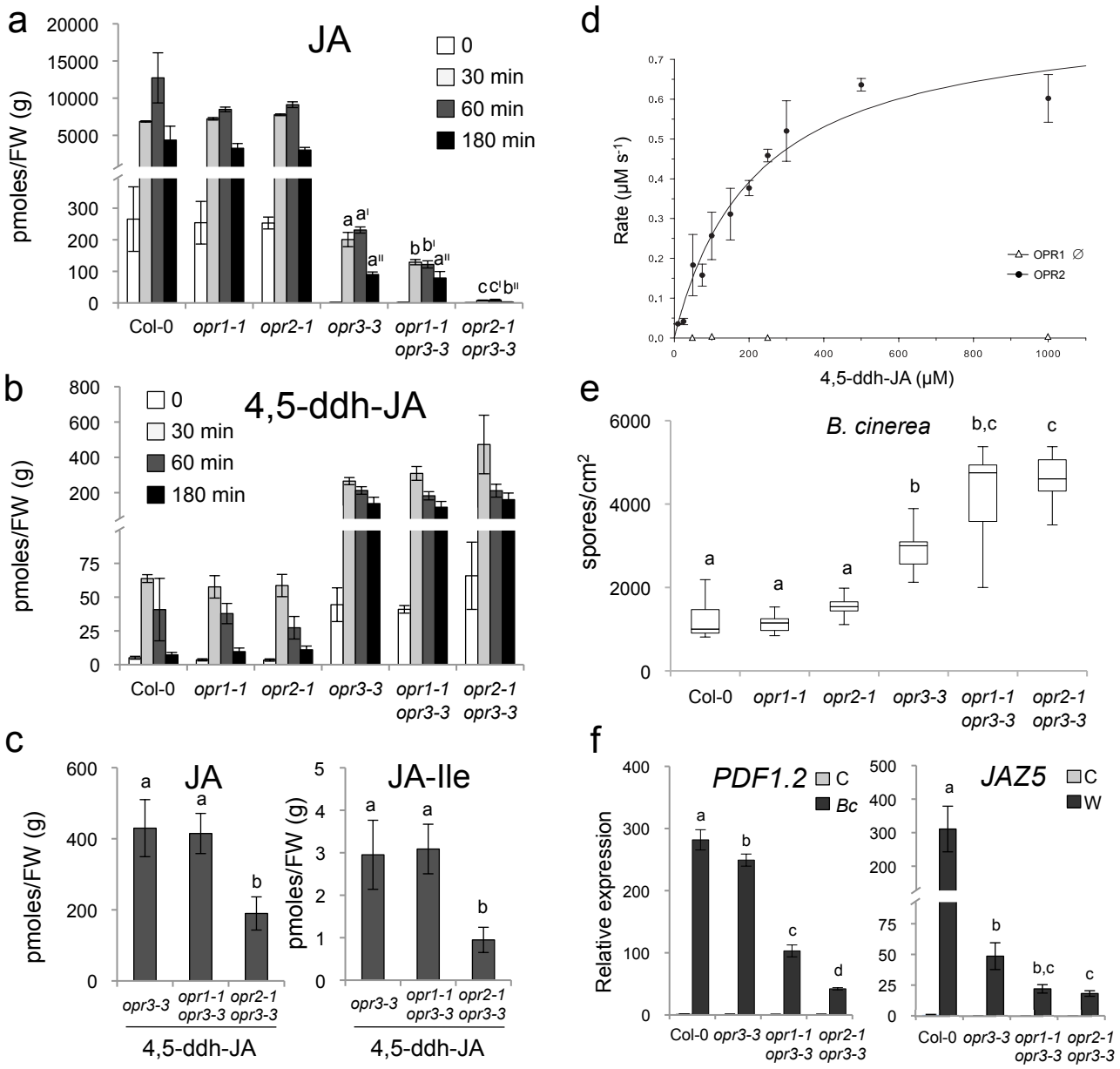

Figure 6. OPR1 and mainly OPR2 convert 4,5-ddh-JA into JA

Supplementary Information

Identification of an OPR3-independent pathway for jasmonate biosynthesis

Andrea Chini[1], Isabel Monte[1], Angel M. Zamarreño[2], Mats Hamberg[3], Steve Lassueur[4], Philippe Reymond[4], Sally Weiss[5], Annick Stintzi[5], Andreas Schaller[5], Andrea Porzel[6], José M. García-Mina[2] and Roberto Solano[1]*

[1] Department of Plant Molecular Genetics, National Centre for Biotechnology, Consejo Superior de Investigaciones Científicas (CNB-CSIC), 28049 Madrid, Spain

[2] Environmental Biology Department, University of Navarra, Navarre, Spain

[3] Division of Physiological Chemistry II, Department of Medical Biochemistry and Biophysics, Karolinska Institutte, Stockholm, Sweden

[4] Department of Plant Molecular Biology, University of Lausanne, CH-1015 Lausanne, Switzerland

[5] Institute of Plant Physiology and Biotechnology, University of Hohenheim, 70593 Stuttgart, Germany

[6] Department of Bioorganic Chemistry, Leibniz Institute of Plant Biochemistry, Halle, Germany.

*Corresponding author: rsolano@cnb.csic.es

Nature Chemical Biology: doi:10.1038/nchembio.2540

Supplementary Results

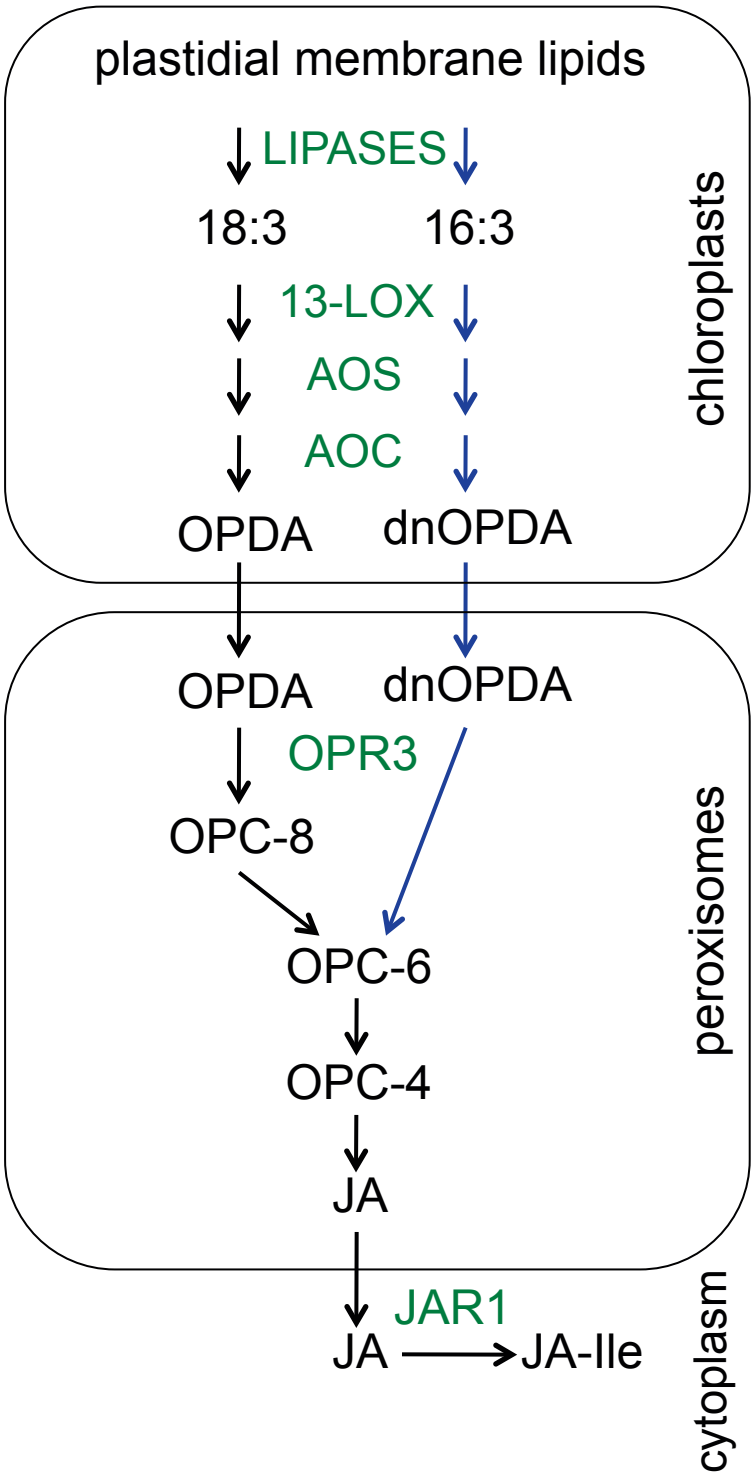

Supplementary Fig. 1. Biosynthesis and intracellular flux of jasmonates in Arabidopsis
Scheme of the biosynthetic pathway of JA-Ile generated from plastidial membrane lipids. Pathway intermediates (described in the text) are 18:3 (α-linolenic acid), 16:3 (hexadecatrienoic acid), OPDA (12-oxo-phytodienoic acid), dnOPDA(dinor-oxo-phytodienoic acid), OPC-8 (8-(3-oxo-2-(pent-2-enyl) cyclopentyl)octanoic acid), OPC-6 (6‑(3-oxo-2-(pent-2-enyl)cyclopentyl)hexanoic acid), OPC-4 (4-(3-oxo-2-(pent-2-enyl)cyclopentyl)butanoic acid), JA (jasmonic acid) and JA-Ile (jasmonoyl-Isoleucine). Black arrows define the octadecanoid pathway, blue arrows indicate the parallel hexadecanoid pathway. Biosynthetic enzymes (described in the text) are shown in green: 13-LOX (13-lipoxygenase), AOS (allene oxide synthase), AOC (allene oxide cyclase), OPR3 (OPDA reductase 3) and JAR1 (jasmonic acid-amido synthetase).

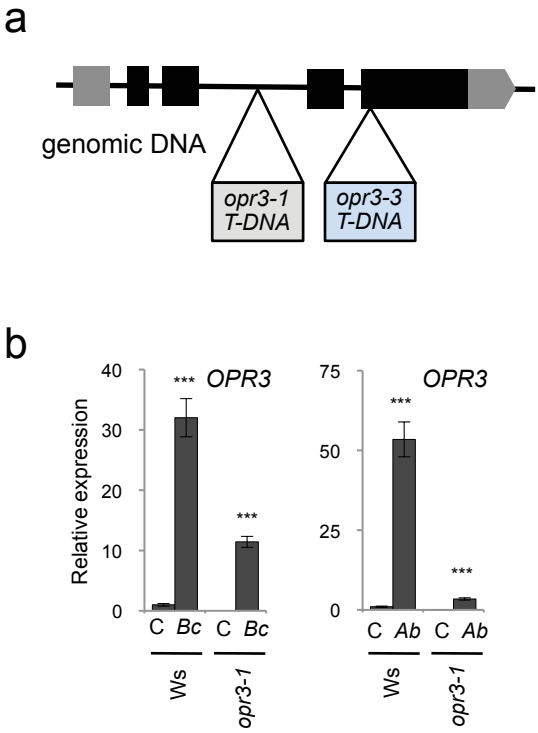

Supplementary Fig. 2. *opr3* mutants in Arabidopsis

(a) Scheme of the *OPR3/AT2G06050* locus, including the T-DNA insertion that defines the *opr3-1* allele [18,33] in Ws accession and *opr3-3* (SK24765) allele in Col-0 accession.

(b) Expression of *OPR3* after fungal infection and wounding of Col-0 and mutant plants (n = 10) measured by real-time PCR in untreated plants (control, C) and plants challenged for 3 days with *B. cinerea* (*Bc*) or 9 days with *A. brassicicola* (*Ab*). Values are the mean ± SD of three technical replicates expressed as relative fold change normalized to *ACT8*. Experiments were repeated twice with similar results. Statistically significant expression compared to untreated plants is highlighted (Student's t-test; ** $p < 0.01$; *** $p < 0.001$).

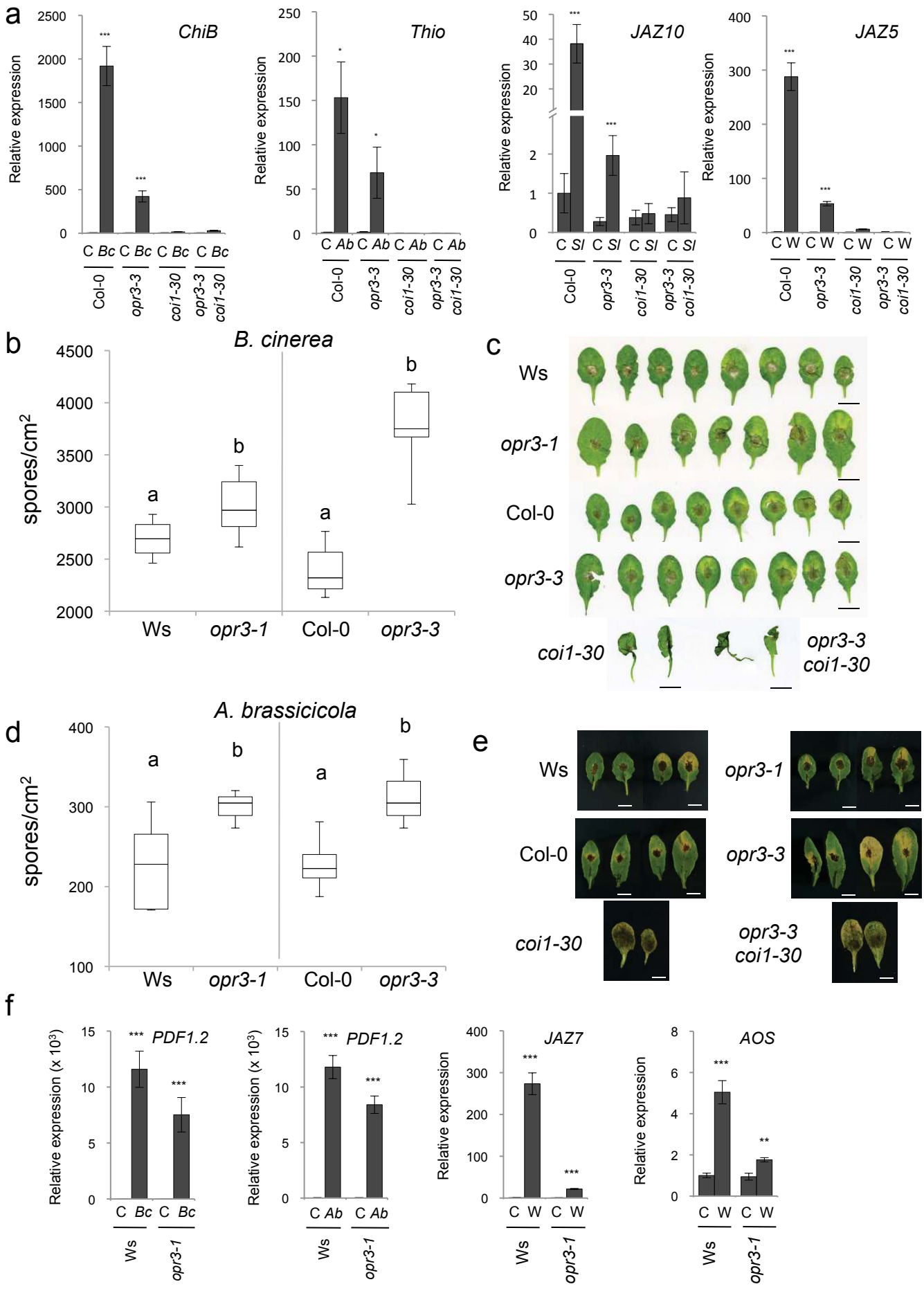

Supplementary Fig. 3. Responses of *opr3* mutants to fungal infection

(a) Expression of JA-regulated genes after fungal infection, insect challenge and wounding of Col-0 and mutant plants (n = 10). *ChiB*, *Thio2.1*, *JAZ10* and *JAZ5* were measured by real-time PCR in untreated plants (control, C) and plants challenged for 3 days with *B. cinerea* (*Bc*) or 9 days with *A. brassicicola* (*Ab*), or 48 h with *S. littoralis* larvae (*Sl*) or 30 min after wounding (W) (n = 10). Values are the mean ± SD of three technical replicates expressed as relative fold change normalized to *ACT8*. Experiments were repeated twice with similar results. Statistically significant wound-induced expression compared to untreated plants are highlighted (Student's t-test; * $p < 0.05$; ** $p < 0.01$; *** $p < 0.001$).
(b and c) Infection of Arabidopsis plants (n = 15) with *B. cinerea*. Quantification of the spores of *B. cinerea* grown on different mutant lines was calculated 72 h post-inoculation. Data shown as box-plots of mean of 5 biological replicates of 5 leaves each. Letters above columns indicate significant differences (one-way ANOVA/post-hoc Tukey HSD Test, $p < 0.05$). The experiment was repeated three times with similar results. Representative leaves of plants infected with *B. cinerea* are shown in (c). Scale bars, 1 cm.
(d and e) Infection of Arabidopsis plants with *A. brassicicola*. Fungal spores, grown on different mutant lines were counted 9 days post-inoculation, are shown as box-plots of mean of 5 biological replicates of 5 leaves each. Letters above columns indicate significant differences (one-way ANOVA/post-hoc Tukey HSD Test, $p < 0.05$). The experiment was repeated three times with similar results. Representative leaves of plants infected with *A. brassicicola* are shown in (e). Scale bars, 1 cm.
(f) Expression of JA-regulated genes after fungal infection and wounding of Col-0 and mutant plants (n = 10). *PDF1.2*, *JAZ7* and *AOS* were measured by real-time PCR in untreated plants (control, C) and plants challenged for 3 days with *B. cinerea* (*Bc*) or 9 days with *A. brassicicola* (*Ab*) or 30 min after wounding (W) (n = 10). Values are the mean ± SD of three technical replicates expressed as relative fold change normalized to *ACT8*. Experiments were repeated twice with similar results. Statistically significant wound-induced expression compared to untreated plants is highlighted (Student's t-test; ** $p < 0.01$; *** $p < 0.001$).

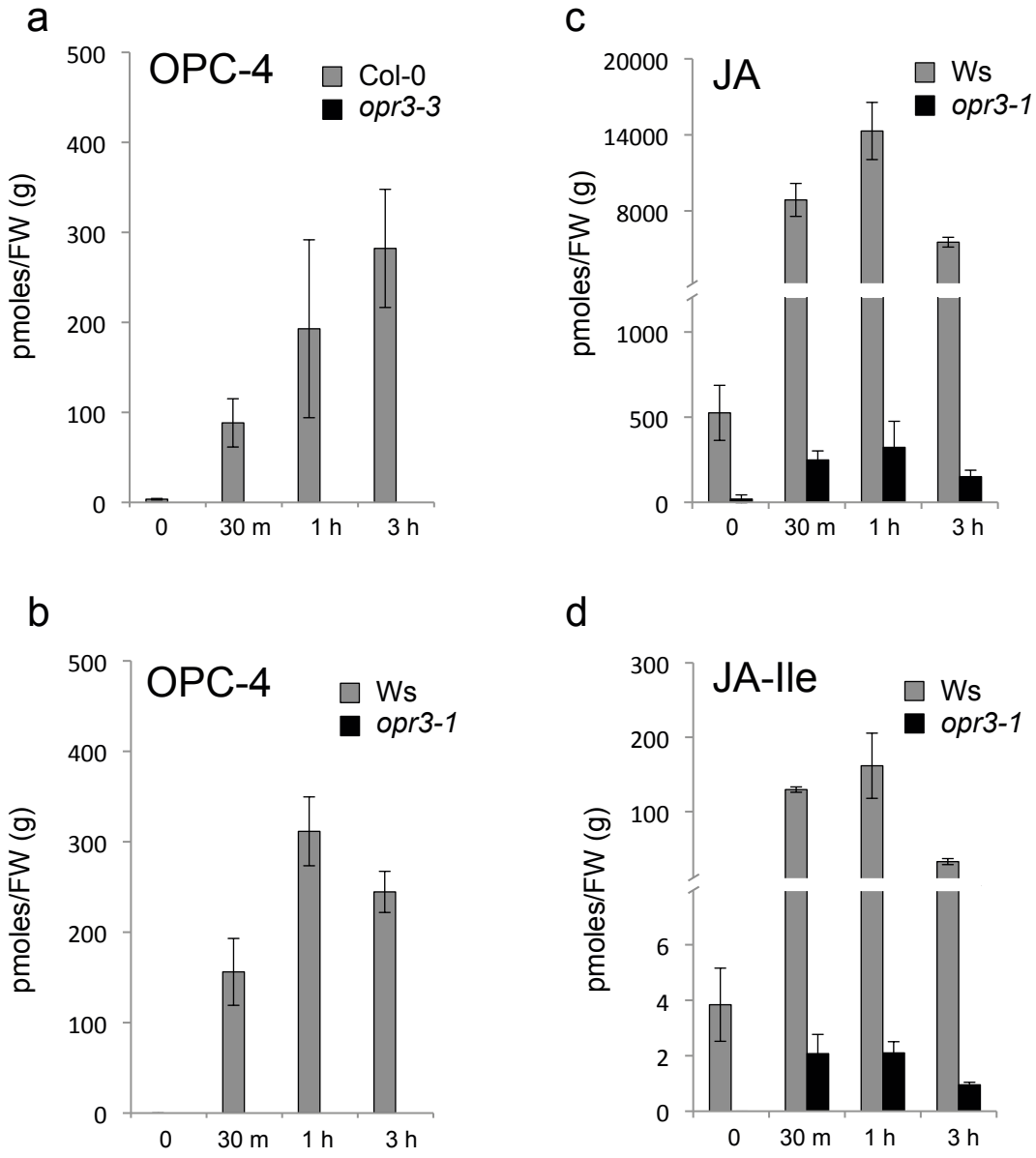

Supplementary Fig. 4. Accumulation of JA derivatives in wild-type plants and *opr3* mutants
Accumulation of OPC-4 (pmoles/fresh weight (g)) (a-b), JA (pmoles/fresh weight (g)) (c) and JA-Ile (pmoles/fresh weight (g)) (d) in wounded wild-type (grey bars) and *opr3* mutants (black bars) plants. Four-week-old plants (n = 10) were wounded and damaged leaves collected at the time indicated. Data for *opr3-3* compared to Col-0 are shown in (a), whereas *opr3-1* compared to Ws is shown in (b) (c) and (d). Data shown as mean ± SD of four biological replicates. The experiment was repeated three times with similar results.

Nature Chemical Biology: doi:10.1038/nchembio.2540

a

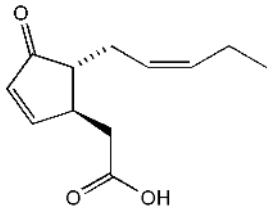

(+)-4,5-ddh-JA (**9**)

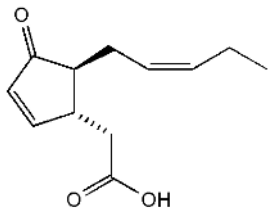

(-)-4,5-ddh-JA (**10**)

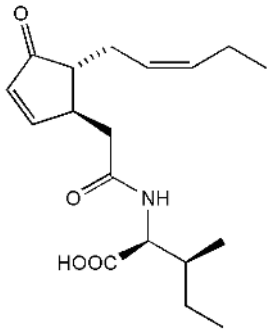

(+)-4,5-ddh-JA-(*S*)-Ile (**11**)

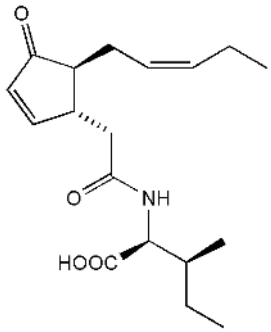

(-)-4,5-ddh-JA-(*S*)-Ile (**12**)

b

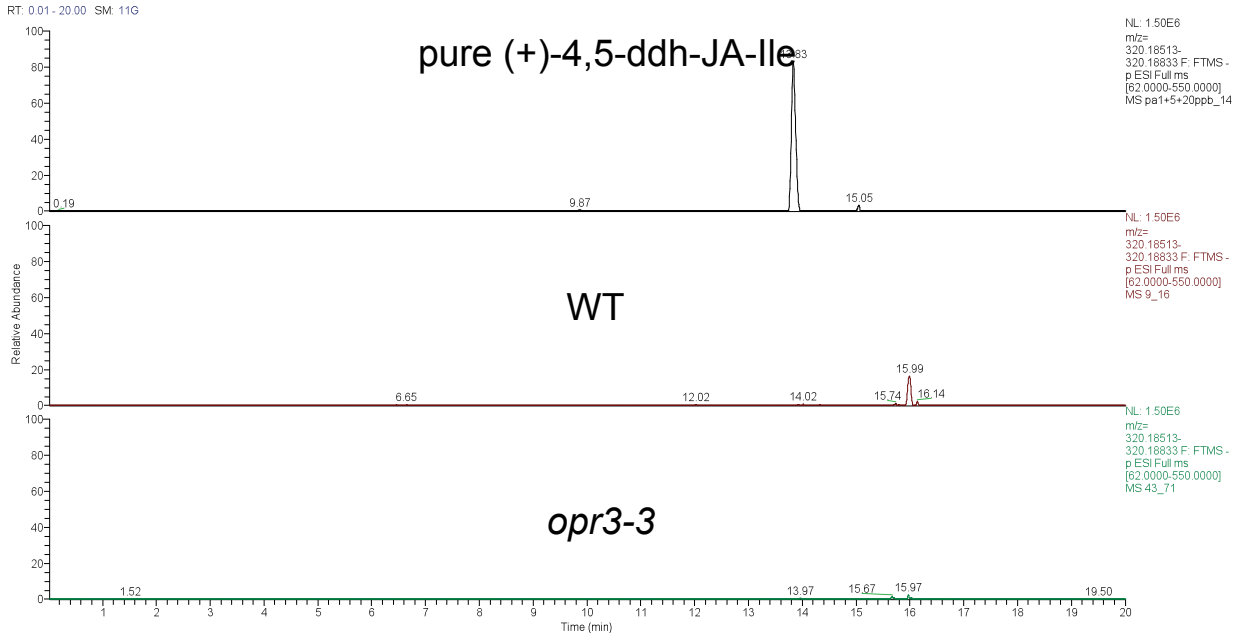

Supplementary Fig. 5. Structures of 4,5-ddh-JA and of 4,5-ddh-JA-Ile
(a) Chemical structures of 4,5-ddh-JA, used as an enantiomeric mixture of the (-)- and (+)-forms, (-)-4,5-ddh-JA-Ile and (+)-4,5-ddh-JA-Ile.
(b) Chromatogram of pure (+)-4,5-ddh-JA-Ile (top panel) and of WT and *opr3-3* plants.

Nature Chemical Biology: doi:10.1038/nchembio.2540

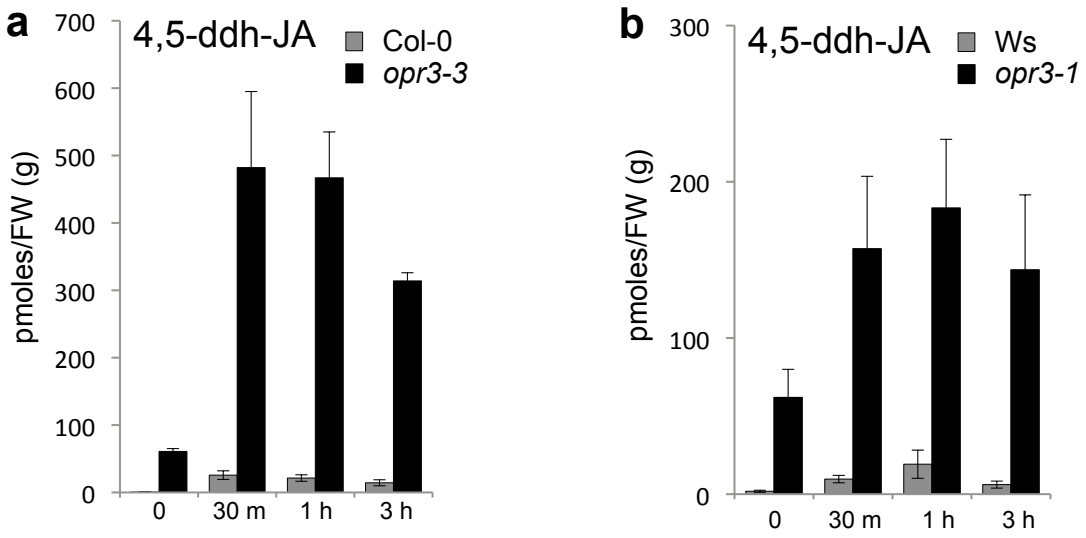

Supplementary Fig. 6. Accumulation of 4,5-ddh-JA in wild-type plants and *opr3* plants
(a and b) Accumulation of 4,5-ddh-JA (pmoles/fresh weight (g)) in wounded wild-type (grey bars) and *opr3* mutants (black bars) plants. Four-week-old plants (n = 10) were wounded and damaged leaves collected at the time indicated. Data for *opr3-3* compared to Col-0 are shown in (a), whereas *opr3-1* compared to Ws are shown in (b). Data shown as mean ± SD of four biological replicates. The experiment was repeated three times with similar results.

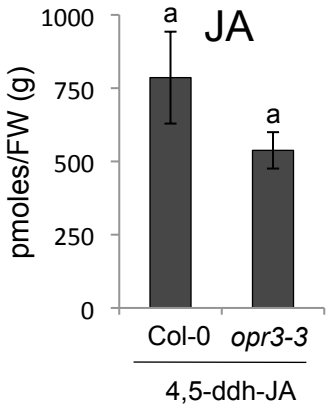

Supplementary Fig. 7. JA accumulation after exogenous 4,5-ddh-JA treatment in Col-0 and *opr3-3* plants. Data shown as mean ± SD of four biological replicates after subtraction of basal JA levels. JA accumulation was not statistically different (Student's t-test $p < 0.01$) in Col-0 compared to *opr3-3* plants ($n = 10$). The experiment was repeated twice with similar results.

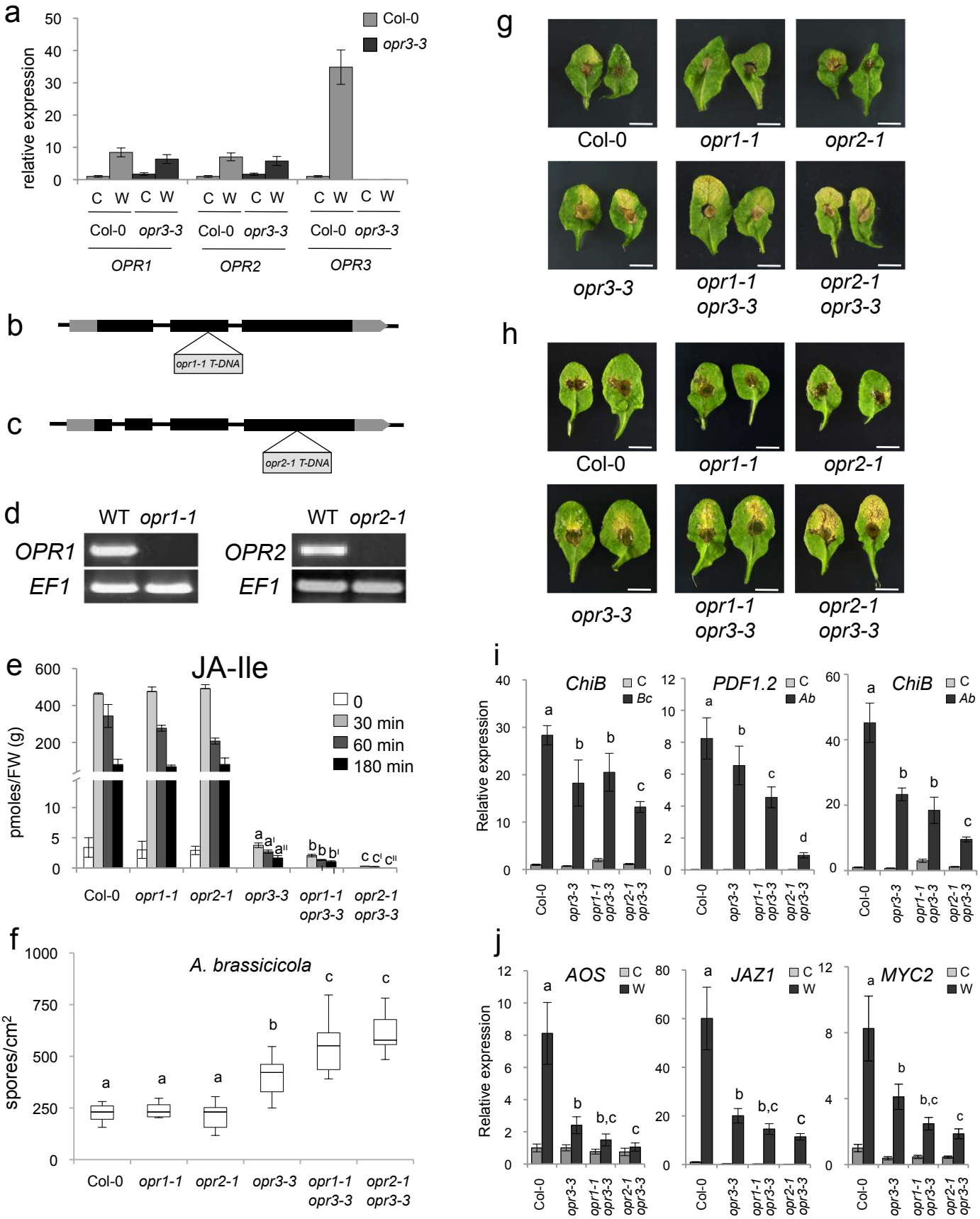

Supplementary Fig. 8. Analysis of *OPR* expression and characterization of *opr* mutants

Nature Chemical Biology: doi:10.1038/nchembio.2540

(a) *OPR1*, *OPR2* and *OPR3* expression in Col-0 and *opr3-3* mutant plants (n = 10) 30 min after wounding (W, dark grey bars). Unwounded plants were included as controls (C, light grey bars). Values are the mean ± SD of three technical replicates expressed as relative fold change normalized to *ACT8*. The experiment was repeated three times with similar results.
(b and c) Genomic scheme of the loss-of-function *opr1-1* (b) (SALK_145353) and *opr2-1* (c) (SALK_116381) mutant lines and the exogenous T-DNA insertions.
(d) Expression analysis by RT-PCR of WT plants and T-DNA insertion lines of *OPR1* and *OPR2* using *EF1* as control transcripts. The experiment was repeated three times with similar results.
(e) Accumulation of JA-Ile (pmoles/fresh weight (g)) in wounded Col-0, *opr* single and double mutant plants (n =10). Five-week-old plants were wounded and damaged leaves collected at time 0 (white bars), 30 (light grey), 60 (dark grey) or 180 min (black) after wounding. Data shown as mean ± SD of four biological replicates. The experiment was repeated three times with similar results.
(f) Box-plots of fungal spore quantification of Col-0 and mutant plants (n = 15) infected with *A. brassicicola* (9 dai). Letters above columns indicate significant differences (one-way ANOVA/post-hoc Tukey HSD Test, $p < 0.01$).
(g-h) Representative leaves of Col-0 and mutant plants infected with *B. cinerea* and *A. brassicicola* are shown in (g) and (h) respectively. Scale bars, 1 cm.
(i) Expression of JA-regulated *ChiB* and *PDF1.2* (in thousands) after fungal infection of Col-0 and mutant plants (n = 10) measured by real-time PCR in untreated plants (control, C) and plants challenged for 7 days with *B. cinerea* (*Bc*) or 9 days with *A. brassicicola* (*Ab*). Values are the mean ± SD of three technical replicates expressed as relative fold change normalized to *ACT8*. Experiments were repeated twice with similar results. Letters above columns indicate significant differences compared to expression in *opr3-3* plants (Student's t-test, $P < 0.05$).
(j) Expression of early JA-regulated genes after wounding in Col-0 and mutant plants (n = 10). *AOS*, *JAZ1* and *MYC2* expression were measured by real-time PCR in untreated plants (control, C, grey bars) and in plants 1 h after wounding (W, dark grey bars). Values are the mean ± SD of three technical replicates expressed as relative fold change normalized to *ACT8*. The experiment was repeated at least twice with similar results. Letters above columns indicate significant differences compared to expression in *opr3-3* plants (Student's t-test, $P < 0.05$).

Supplementary Table 1
List of primers used

Name	Sequence
OPR1 qPCR-F	5'-ATCCAGGAGCATTAGGGCT-3'
OPR1 qPCR-R	5'-CGCTTTCCTCATCGGCAT-3'
OPR2 qPCR-F	5'-TCCAGAAGCATTAGGGCTGT-3'
OPR2 qPCR-R	5'-TGATGTTGAAAGCACATATAAAAGC-3'
OPR3-3 qPCR-F	5’-GCATGGAAGCAAGTTGTGGAAGCA-3’
OPR3-3 qPCR-R	5'-CATGCGCCCCGTGGATCTCAAT-3’
OPR3-3 qPCR-F2	5'-ATCTCTCTCATCGAGTGGTT-3'
OPR3-3 qPCR-R2	5'-CCTCCATTAGGTTGATACACTG-3'
PDF1.2 qPCR-F	5’-CACCCTTATCTTCGCTGCTC-3’
PDF1.2 qPCR-R	5’-GTTGCATGATCCATGTTTGG-3’
CYP79B3 qPCR-F	5'-CTTTGCTTACCGCTGATGAA-3'
CYP79B3 qPCR-R	5'-GCGTTTGA TGGGTTGTCTG-3'
AOS qPCR-F	5'-GCGACGAGAGATCCGAAGA-3'
AOS qPCR-R	5'-CTCGCCACCAAAACAACAAA -3'
LOX3 qPCR-F	5'-CACTGCAATTCACAAGCAACC-3'
LOX3 qPCR-R	5'-CAAAGGAGGAATCGGAGAAGC-3'
JAZ1 qPCR-F	5'-CACGTCTGTGAGAAGCTAGGC-3'
JAZ1 qPCR-R	5'-TTCTGAGTTCGTCGGTAGCC-3'
JAZ5 qPCR-F	5'-AAAGATGTTGCTGACCTCAGTG-3'
JAZ5 qPCR-R	5'-CCCTCCGAAGAATATGGTCA-3'
JAZ7 qPCR-F	5'-TTCGGATCCTCCAACAATCCCA-3'
JAZ7 qPCR-R	5'-TCAAGACAATTGGATTATTATGTTACAGT-3'
MYC2 qPCR-F	5'-GTGCGGGATTAGCTGGTAAA-3'
MYC2 qPCR-R	5'-ATGCATCCCAAACACTCCTC-3'
ACT8 qPCR-F	5'-CCAGTGGTCGTACAACCGGTA-3'
ACT8 qPCR-R	5'-TAGTTCTTTTCGATGGAGGAGCTG-3'
Name	Sequence
LB_GW1	5'-GCTTTCGCCTATAAATACGACGGATCGT-3'
SLBb1.3	5'-ATTTTGCCGATTTCGGAAC-3'
OPR1_F1	5'-AACACACTACATTACATTATTGATAACA-3'
OPR2_F1	5'-GAAACACATTACATTACTGATAACACGA-3'
OPR3_F1	5'-GCATGGAAGCAAGTTGTGGAAGCA-3'

Supplementary Table 2
Ionization source working parameters

Instrumental parameters	Value
Sheath gas flow rate	44 au
Auxiliary gas flow rate	11 au
Sweep gas flow rate	1 au
Spray voltage	3.5 kV
Capillary temperature	340 ºC
S-lens RF level	50
Auxiliary gas heater temperature	300 ºC

Supplementary Table 3
Masses of phytohormones and internal standard and their principal fragments

Analyte	$[M-H]^{-1}$ Phytohormone
JA	209.11832
Ja-Ile	322.20238
OPDA	291.19657
dn-OPDA	263.16527
4,5-ddh-JA	207.10267
4,5-ddh-JA-Ile	320.18673
OPC-4	237.14962
OPC-6	265.18092
$^{2}H_5$-JA	214.1497
$^{2}H_5$-JA-Ile	327.23377
$^{2}H_5$-OPDA	296.22795
$^{2}H_5$-dnOPDA	268.19665
$^{2}H_5$-tnOPDA	235.13397
$^{2}H_5$-4,5-ddh-JA	212.13405
$^{2}H_5$-ddh-JA-Ile	325.21812
$^{2}H_5$-OPC-4	242.181
$^{2}H_5$-OPC-6	270.2123
$^{2}H_5$-JA	214.1497
$^{2}H_5$-JA-Ile	324.21494
$^{2}H_5$-OPDA	296.22795
$^{2}H_5$-dnOPDA	268.19665

Analyte	$[M-H]^{-1}$ Fragment
JA	59.01297
Ja-Ile	130.08735
OPDA	165.12843
dn-OPDA	165.12843
4,5-ddh-JA	163.11282
4,5-ddh-JA-Ile	130.08735
OPC-4	125.09715
OPC-6	96.95968
$^{2}H_5$-JA	61.02555
$^{2}H_5$-OPDA	170.15994
$^{2}H_5$-dnOPDA	170.15994
$^{2}H_5$-JA	61.02555
$^{2}H_5$-JA-Ile	131.0937
$^{2}H_5$-OPDA	170.15994
$^{2}H_5$-dnOPDA	170.15994

Supplementary Note 1

Chemical synthesis

Analytical and chromatographical methods. Gas chromatography-mass spectrometry (GC-MS) was carried out using an Agilent mass selective detector model 5977E connected to an Agilent model 7820A gas chromatograph. A capillary column of 5% phenylmethylsiloxane (12 m, 0.33 μm film thickness) with helium as the carrier gas was used. The temperature was raised from 80°C to 320°C at a rate of 10°C/min. Reversed-phase HPLC (RP-HPLC) was carried out using a column of 250 x 10 mm Nucleosil 100-7 C_{18} eluted with methanol-water-acetic acid (55:45:0.02, v/v/v) at a flow rate of 4 mL/min, whereas straight-phase HPLC (SP-HPLC) was performed with a column of Nucleosil 50-7 (250 x 10 mm) using the solvent systems indicated at a flow rate of 4 mL/min. NMR spectra were recorded on $CDCl_3$ solutions using Bruker 500 or 600 MHz instruments.

Chemicals. Methyl (±)- jasmonate, L-isoleucine and all other chemicals used were purchased from Sigma-Aldrich.

*Methyl (±)-4,5-didehydrojasmonate (**13**)*. The title compound was prepared by modification of a previously described protocol [54]. Thus, methyl (±)-jasmonate (1 mmol, 224 mg) was added to dry *N,N*-dimethylformamide (3 mL) containing diethyl allyl phosphate (2 mmol, 388 mg), Na_2CO_3 (2.4 mmol, 254 mg) and palladium(II) acetate (0.12 mmol, 27 mg). The solution was purged with argon and stirred at 80°C for 24 h. Water was added and the mixture extracted with diethyl ether. After drying over $MgSO_4$ the solvents were evaporated leaving a residue of 250 mg. Purification was performed on a silica gel column (5 g) which was eluted with diethyl ether/hexane (1:9, v/v), 15 fractions of 15 mL. Unreacted methyl jasmonate was

recovered in fractions 5-7 and methyl 4,5-ddh-JA was present in fractions 9-14. The latter were combined and evaporated, leaving 76 mg of the title compound (yield, 34%) accompanied by 4 mg of an unknown allyl adduct of methyl 3,7-ddh-JA and traces of methyl 7,8-ddh-JA and methyl 3,7-ddh-JA. Preparative SP-HPLC using a solvent system of 2-propanol-hexane (1:99, v/v) afforded the pure title compound as a colorless oil. The mass spectrum showed prominent ions at *m/z* 222 (30%, M^+), 193 (15, $M^+ - C_2H_5$), 167 (13), 154 (70, rearrangement with loss of the C-8 to C-12 side chain), 133 (30), 107 (25), and 95 (100). The UV spectrum (EtOH) showed λ_{max} 217 nm and the ^{1}H NMR spectrum showed signals at δ 0.98 (3H, t, J = 7.5 Hz), 2.05-2.14 (3H, m), 2.30-2.37 (1H, m), 2.49 (1H, dd, J = 15.8, 8.3 Hz), 2.50-2.58 (1H, m), 2.60 (1H, dd, J = 15.8, 6.7 Hz), 3.00-3.06 (1H, m), 3.72 (3H, s), 5.28 (1H, dtt, J = 10.8, 7.5, 1.7 Hz), 5.49 (1H, dtt, J = 10.8, 7.4, 1.7 Hz), 6.20 (1H, dd, J = 5.8, 2.0 Hz), and 7.64 (1 H, dd, 5.8, 2.4 Hz). This spectrum was in full agreement with that previously published [54].

*Methyl (+)-(3S,7R)-4,5-didehydrojasmonate (**14**)*. The (+)-rotatory form of the side chain *trans* isomer of methyl 4,5-didehydrojasmonate is the 3S,7R enantiomer [55] and is the form which is stereochemically related to natural methyl (-)-jasmonate (3R,7R). It should be noted that introduction of the ring double bond reverses the sign of optical rotation and that the change in configurational assignment at C-3 is a consequence of the Cahn-Ingold-Prelog rules. In the present work, the title compound was prepared by palladium-catalyzed dehydrogenation of the methyl ester of (-)-JA (22 mg), which was available since a previous study [56]. The material obtained (9 mg) showed λ_{max} (EtOH) 217 nm and the mass spectrum was identical to that given above for the (±) form.

*(±)-4,5-Didehydrojasmonic acid (**6**).* Methyl (±)-4,5-didehydrojasmonate (100 mg, 0.45 mmol) was added to a solution of 24 mg of LiOH (1 mmol) in 6 mL of water and 24 mL of tetrahydrofuran. The solution was stirred at 23°C for 18 h. The product obtained following extraction with diethyl ether was subjected to preparative SP-HPLC using a solvent system of 2-propanol-hexane-acetic acid (4:96:0.02, v/v/v). This provided the pure title compound as a colorless oil (59 mg) showing λ_{max} 217 nm. The mass spectrum of a methyl-esterified sample was identical to that of methyl 4,5-ddh-JA, and the mass spectrum of the trimethylsilyl (Me_3Si) ester derivative showed prominent ions at *m/z* 280 (22%, M^+), 251 (7, M^+ - C_2H_5), 212 (18, rearrangement with loss of the C-8 to C-12 side chain), 148 (21), 117 (15, $O{=}C{=}O^+SiMe_3$) and 73 (100, Me_3Si^+).

*(+)-(3S,7R)-4,5-Didehydrojasmonic acid (**9**).* Methyl (+)-4,5-didehydrojasmonate (9 mg, 0.04 mmol) was treated with LiOH (2.4 mg, 0.1 mmol) using the above-described protocol. The pure title compound was obtained following SP-HPLC as described above. Its properties including the UV spectrum and mass spectrum were identical to those recorded for the racemic compound.

*Coupling of (±)-4,5-didehydrojasmonic acid (**6**) to (S)-isoleucine*. (±)-4,5-Didehydrojasmonic acid (90 mg, 433 μmol) was dissolved in 18 mL of redistilled ethyl acetate containing 9.8 mg (97 μmol) triethylamine. *O*-(Benzotriazol-1-yl)-*N,N,N′,N′*-tetramethyluronium tetrafluoroborate (TBTU, 161 mg, 501 μmol) was added and the solution stirred at 23°C for 30 min. (*S*)-Isoleucine (171 mg, 1303 μmol) suspended in 9 mL of dry *N,N*-dimethylformamide was added and the mixture stirred at 23°C for 18 h. Extraction with ethyl acetate at pH 2 afforded a product that was purified on a silica gel column (5 g). Elution with ethyl acetate/chloroform/acetic acid

(4:6:0.05, v/v/v) afforded a diasteromeric mixture of comparable amounts of the (*S*)-isoleucine conjugates of (+)- and (-)-4,5-ddh-JA. These were resolved by preparative RP-HPLC which afforded an earlier eluting and a later eluting conjugate (retention volumes, 86 and 104 mL, respectively). The methyl esters of these diastereomers showed a small separation on GC-MS analysis where, under the conditions used, the earlier-eluting and later-eluting conjugates had retention times of 16.68 and 16.74 min, respectively.

In view of previous data recorded for the (+)- and (-) (*S*)-isoleucine conjugates of (±)-JA [8], the results suggested that the earlier and later eluting 4,5-ddh-JA conjugates obtained as described above were the (-)- and (+)-isomers, respectively. In order to firmly establish this point a separate experiment was conducted in which (+)-4,5-ddh-JA (5 mg) was coupled to (*S*)-isoleucine. Analysis of the product using RP-HPLC showed a single peak which matched that ascribed to the (+) conjugate obtained from (±)-4,5-ddh-JA, thus unequivocally showing that the diastereomer that eluted faster on RP-HPLC was the (-)- or (3R,7S) isomer, whereas the slower-eluting diastereomer was the (+)- or (3S,7R) isomer.

*N-[(+)-(3S,7R)-4,5-didehydrojasmonoyl]-(S)-isoleucine (**11**).* The above-mentioned later eluting (*S*)-isoleucine conjugate (16 mg) was a colorless semisolid whose UV spectrum (EtOH) showed λ_{max} 217 nm (ε 10,800). An aliquot was dissolved in 50 μL of methanol and treated with diazomethane and taken to dryness after about 5 s (longer times of treatment led to the formation of byproducts). Analysis by GC-MS showed a single peak and the mass spectrum showed prominent ions at *m/z* 335 (27%, M^+), 306 (16, M^+ - C_2H_5), 276 (22, M^+ - CH_3COO), 190 (11, M^+ - [NH-CH($OOCCH_3$)-C_4H_9 + H]), 146 (44, [NH-CH($OOCCH_3$)-C_4H_9 + 2 H]), 128 (34, [CH($OOCCH_3$)-C_4H_9 - H]), and 86 (100, 146 - CH_3COOH). The structure (Suppl.

Figure 5a) was fully supported by the ^{1}H and ^{13}C NMR spectra (Supplementary Note Table 1).

*N-[(-)-(3R,7S)-4,5-didehydrojasmonoyl]-(S)-isoleucine (**12**).* The earlier eluting (*S*)-isoleucine conjugate (15 mg) showed λ_{max} 217. An aliquot was treated with diazomethane (5-10 s) and gave a single peak on GC-MS. The mass spectrum was virtually identical to that of the (+)-conjugate. The structure (Supplementary Fig. 5a) was fully supported by the ^{1}H and ^{13}C NMR spectra (Supplementary Note Table 2).

*Alkali-promoted cyclization of N-[(+)-(3S,7R)-4,5-didehydrojasmonoyl]-(S)-isoleucine (**11**).* A sample of *N*-[(+)-4,5-didehydrojasmonoyl]-(*S*)-isoleucine (34 mg) was dissolved in methanol (4.5 mL) and 2 M NaOH in water (0.5 mL) was added. The solution was kept at 23°C for 1 h and then acidified and extracted with ethyl acetate. The product was purified by RP-HPLC, which showed a main peak at a retention volume of 100 mL. This material was subjected to SP-HPLC using a solvent system of ethanol-hexane-acetic acid (5:95:0.1, v/v/v). Two peaks appeared, *i.e.* cyclization product (CP)-1 (**15**) (5 mg; 60 mL effluent) and CP-2 (**16**) (17 mg; 76 mL effluent) (Supplementary Note Fig. 1). The UV spectra of these two materials lacked the absorption band present in the parent compound, thus indicating the disappearance of the conjugated ring double bond.

*Cyclization product-2 (**16**).* GC-MS analysis of the methyl ester of CP-2 showed prominent ions at *m/z* 335 (10%, M^+), 306 (5, $M^+ - C_2H_5$), 279 (30, $M^+ - C_4H_8$), 276 (100, $M^+ - COOCH_3$), 250 (26, 306 - C_4H_8), 247 (24, 306 - $COOCH_3$) and 208 (21). This spectrum combined with the lack of the ring double bond as indicated by UV spectroscopy suggested a bicyclic structure in which the nitrogen atom of the isoleucine residue had attacked C-4 of the didehydrojasmonoyl residue (Supplementary Note Fig. 1). An alternative reaction involving Michael attack by the

α carbon anion of the isoleucine moieity on C-4 could be ruled out by NMR spectrometry (Supplementary Note Table 3).

*Cyclization product.1 (**15**).* On GC-MS, the methyl ester of CP-1 eluted somewhat later compared to CP-2 (retention times, 16.8 and 16.1 min, respectively). Its mass spectrum was similar to that of the methyl ester of CP-2 and showed prominent ions at *m/z* 335 (8%, M^+), 306 (2, M^+ - C_2H_5), 279 (22, M^+ - C_4H_8), 276 (100, M^+ - $COOCH_3$), 250 (5, 306 - C_4H_8), 247 (12, 306 - $COOCH_3$) and 208 (15). Treatment of CP-1 with NaOH produced an equilibrium mixture of CP-2 and CP-1 in proportions about 3:1, thus indicating that the 2(*Z*)-pentenyl side chain is *cis*-oriented with respect to the amide ring in CP-1 and *trans*-oriented in CP-2 (Supplementary Note Fig. 1).

Supplementary Note Table 1

NMR data of (+)-4,5-didehydro-JA-Ile (solvent: $CDCl_3$)

Pos.	δ ^{13}C [ppm]	^{13}C mult.	δ ^{1}H [ppm] mult. (J[Hz]]
1	170.7	s	-
2	40.5	t	2.543 dd (14.5;6.5) / 2.360 dd (14.5;8.6)
3	43.9	d	3.097 m
4	166.2	d	7.700 dd (5.8;2.4)
5	133.6	d	6.183 dd (5.8,2.0)
6	210.7	s	-
7	51.0	d	2.08
8	27.8	t	2.518 m / 2.314 br dt (14.4;7.3)
9	124.5	d	5.276 dtt (10.8;7.5;1.6)
10	134.6	d	5.475 dtt (10.8;7.3;1.5)
11	20.6	t	2.066 dqd (7.4;7.4;1.6)
12	14.2	q	0.959 t (7.6)
1’	56.4	d	4.630 dd (8.4;4.8)
2’	37.4	d	2.066 dqd (7.4;7.4;1.6)
3’	25.1	t	1.496 dqd (13.6;7.5;4.6) / 1.213 m
4’	11.6	q	0.954 t (7.5)
5	15.5	q	0.969 d (6.8)
6’	174.8	s	-
NH	-	-	6.027 d (8.4)

^{1}H chemical shifts with only two decimal places are chemical shifts of HSQC correlation peaks

Supplementary Note Table 2

NMR data of (-)-4,5-didehydro-JA-Ile (solvent: $CDCl_3$)

Pos.	δ ^{13}C [ppm]	^{13}C mult.	δ ^{1}H [ppm] mult. (J[Hz]]
1	170.6	s	-
2	40.4	t	2.518 dd (14.6;6.9) / 2.395 dd (14.6;8.2)
3	43.8	d	3.097 m
4	166.2	d	7.661 dd (5.7;2.4)
5	133.6	d	6.182 dd (5.7,2.0)
6	210.8	s	-
7	51.0	d	2.101 ddd (7.8;4.7;2.4)
8	27.8	t	2.507 m / 2.312 br dt (14.5;7.8)
9	124.4	d	5.249 dtt (10.8;7.5;1.5)
10	134.6	d	5.464 dtt (10.8;7.3;1.4)
11	20.6	t	2.059 dqd (7.4;7.4;1.5)
12	14.2	q	0.953[a] t (7.6)
1’	56.4	d	4.653 dd (8.5;4.7)
2’	37.5	d	1.971 m
3’	25.1	t	1.494 dqd (13.6;7.5;4.5) / 1.215 ddq(13.6;9.3;7.5)
4’	11.6	q	0.952[a] t (7.6)
5’	15.5	q	0.970 d (6.8)
6’	175.1	s	-
NH	-	-	6.066 d (8.6)

[a] may be interchanged

Supplementary Note Table 3

NMR data of CP-2 methyl ester (solvent: $CDCl_3$)

Pos.	δ ^{13}C [ppm]	^{13}C mult.	δ ^{1}H [ppm] mult. (J[Hz]]
1	174.9	s	-
2	37.0	t	2.71 / 2.390 m
3	38.7	d	2.68
4	58.0	d	4.301 td (7.2; 3.4)
5	43.4	t	2.71 / 2.541 dd (19.3; 7.2)
6	216.3	s	-
7	53.1	d	2.184 m
8	27.0	t	2.450 m / 2.274 dtd-like (14.4;8.1;1.2)
9	124.0	d	5.256 dtt (10.8;7.6;1.6)
10	134.9	d	5.520 dtt (10.8;7.4;1.4)
11	20.6	t	2.046 dqd (7.6;7.6;1.6)
12	14.1	q	0.956 (7.6)
Me	52.0	q	3.715 (s)
1´	60.4	d	4.318 d (10.6)
2´	35.2	d	2.03
3´	25.1	t	1.373 dqd (13.7;7.4;3.1) / 1.054 ddq (13.7;9.7;7.4)
4´	10.8	q	0.871 t (7.6)
5´	16.3	q	0.950 d (6.6)
6´	170.4	s	-

^{1}H chemical shifts with only two decimal places are chemical shifts of HSQC correlation peaks

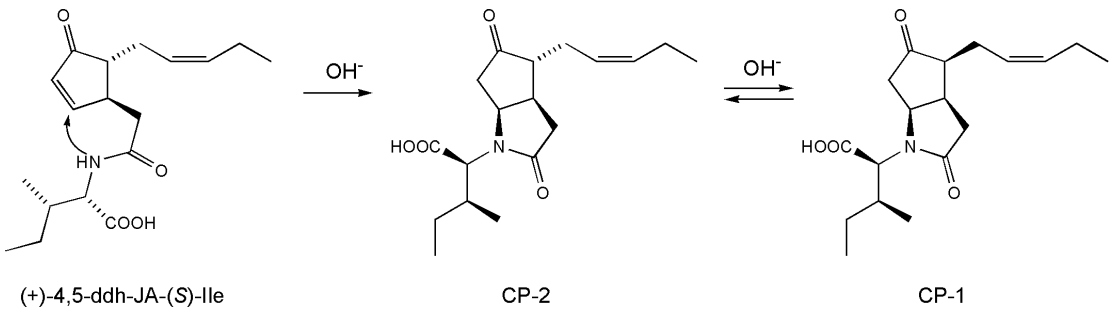

(+)-4,5-ddh-JA-(*S*)-Ile CP-2 CP-1

Supplementary Note Figure 1.

(+)-4,5-didehydrojasmonoyl]-(*S*)-isoleucine (**11**), CP-2 (**16**) and CP-1 (**15**)

Alkali-promoted conversions of N-[(+)-4,5-didehydrojasmonoyl]-(*S*)-isoleucine showing attack by the isoleucine nitrogen at C-4 of the didehydrojasmonoyl residue. The primary product CP-2 is in base-catalyzed equilibrium with CP-1, in which the 2(Z)-pentenyl side chain of the jasmonoyl residue is cis-oriented with respect to the amide ring.

Supplementary Note References

8 Fonseca, S. *et al.* (+)-7-iso-Jasmonoyl-L-isoleucine is the endogenous bioactive jasmonate. *Nat Chem Biol* **5**, 344-350, doi:10.1038/nchembio.161 (2009).

54 Schaller, F. & Weiler, E. W. Molecular cloning and characterization of 12-oxophytodienoate reductase, an enzyme of the octadecanoid signaling pathway from *Arabidopsis thaliana*. Structural and functional relationship to yeast old yellow enzyme. *J. Biol. Chem.* **272**, 28066-28072 (1997).

55 Asamitsu, Y., Nakamura, Y., Ueda, M., Kuwahara, S. & Kiyota, H. Synthesis and odor description of both enantiomers of methyl 4,5-didehydrojasmonate, a component of jasmin absolute. *Chem Biodivers* **3**, 654-659, doi:10.1002/cbdv.200690068 (2006).

56 Suza, W. P., Rowe, M. L., Hamberg, M. & Staswick, P. E. A tomato enzyme synthesizes (+)-7-iso-jasmonoyl-L-isoleucine in wounded leaves. *Planta* **231**, 717-728, doi:10.1007/s00425-009-1080-6 (2010).